UNIVERSITY OF CALIFORNIA SAN DIEGO

# Flexible entrainment of peripheral clock gene expression rhythms via unconventional waveform manipulation

A Thesis submitted in partial satisfaction of the requirements
for the degree Master of Science

in

Biology

by

Alexandra Koretoff

Committee in charge:

Professor Michael Gorman, Chair
Professor Susan Golden, Co-Chair
Professor Stuart Brody

2022

The Thesis of Alexandra Koretoff is approved, and it is acceptable in quality and form for publication on microfilm and electronically.

University of California San Diego

2022

TABLE OF CONTENTS

LIST OF FIGURES

LIST OF TABLES

ACKNOWLEDGEMENTS

To my thesis advisor, Michael Gorman, thank you so much for helping mold me into a more inquisitive scientist and independent thinker. Aside from all of the circadian disruption I incurred from middle-of-the-night feeder checks, my experience in the Gorman Lab has been wonderful and fruitful.

Thank you to the other members of my thesis committee, Susan Golden and Stuart Brody, for their support and roles in fostering my interest in studying peripheral gene expression rhythms.

I would also like to thank the other research assistants of the Gorman Lab for all of their efforts that contributed to the completion of my thesis. Special thanks to Karen Tonsfeldt, who encouraged and guided me through learning all of the necessary molecular techniques I needed to complete this project.

Thank you to Pamela Mellon, who generously allowed me to utilize lab space and equipment.

Lastly, I would like to thank my family and friends for their support and encouragement, as well as my peers in the Biology Graduate program.

.

Chapter 2, in part is currently being prepared for submission for publication of the material. Harrison, Elizabeth; Koretoff, Alexandra. The thesis author was the primary researcher and author of this material.

Chapter 3, in part is currently being prepared for submission for publication of the material. Koretoff, Alexandra. The thesis author was the primary researcher and author of this material.

VITA

2020 Bachelor of Science in Human Biology, University of California San Diego

2022 Master of Science in Biology, University of California San Diego

ABSTRACT OF THE THESIS

Enhancement of Circadian Flexibility Via Unconventional Waveform Manipulation

by

Alexandra Koretoff

Master of Science in Biology
University of California San Diego, 2022

Professor Michael Gorman, Chair
Professor Susan Golden, Co-Chair

Over time, the mammalian circadian system has evolved to anticipate a 24 hour day. These rhythms are robust and not easily perturbed, but as a consequence, are also difficult to reset. Until the modernization of society and the advent of artificial light, the inability to reset rhythms has not been a problem. This inflexibility has the potential to induce health complications like mental illness and metabolic dysfunction when there is desynchrony between internal rhythms and the outside world is chronic, such as in shift workers whose schedules do not align with a normal day. Studies on the flexibility

of circadian rhythms have mainly focused on standard 24 hour entrainment paradigms, but few have considered how plasticity may change under non-standard environmental conditions.

Chapter 2 introduces the idea that bifurcation of circadian waveforms in peripheral tissues induces extraordinary flexibility in clock gene expression rhythms when challenged with simulated jet-lag. Bifurcated clock gene expression rhythms are low amplitude, which may enable such rapid resetting in peripheral tissues. Chapter 3 describes that the implementation of an 18 hour light and food restricted schedule can, remarkably, entrain low amplitude hepatic clock gene expression rhythms to an 18 hour day (T18). Entrainment to T18 is well beyond the established limits of entrainment for the liver (T=22-26 hours), and was not achieved in previous studies on T18 photoperiod without time restricted eating.

Together, this thesis demonstrates increased circadian plasticity of mammalian peripheral clock gene expression rhythms beyond what was previously thought to be possible under standard environmental conditions. Enhanced flexibility of entrainment may be due to low amplitude clock gene expression rhythms, but the mechanism remains unknown. These results broaden the understanding of circadian flexibility and provide insight on mitigation of circadian disruption.

# Chapter 1: General Introduction

Rhythmic phenomena exist in the natural world in and around us, such as tidal patterns and photoperiodism. Biological rhythms, like the sleep/wake cycle, that align with 24 hour geophysical rhythms are considered circadian, and are endogenously generated and self-sustained (Duffy, 2009). Circadian rhythms are generated by complex, cell-autonomous time-keeping systems within the body and consist of the central oscillators and the individual clocks that exist within peripheral cells. These cellular clocks run on a near 24 hour loop that is driven by a transcription-translation feedback loop involving the core clock proteins PER, CRY, BMAL1, and CLOCK. Additionally, this feedback loop's robust rhythm is stabilized by a secondary loop involving BMAL1, RORα, and REV-ERBα and β. BMAL1 and CLOCK are transcription factors that dimerize and promote the expression of PER and CRY. Increased levels of PER and CRY undergo nuclear translocation, where they induce epigenetic changes that repress the action of BMAL1 and CLOCK (Dunlap, 1999; Reppert, 2001). The phase of clock gene expression is paced by central oscillators, such as the suprachiasmatic nuclei (SCN), that integrate timing cues from the external environment (Ralph, 1988). Because we live in a world where many of the major zeitgebers cycle on a 24 hour basis, most of the exploration into circadian rhythms has focused on rhythms with 24 hour periodicity.

As our society advances technologically, we move further and further away from rhythms aligned to the 24 hour day. Artificial lighting and electronic devices all emit signals that influence our circadian system, and can negatively impact human health. Introduction of stimuli at the wrong time can cause a delay or advance in biological

rhythms, which moves said rhythm further from alignment to the external environment (Snyder, 2019). This is referred to as circadian desynchrony, and occurs due to relative inflexibility of circadian rhythms (Potter, 2016). Generally, rhythms of a circadian nature are capable of resetting their rhythms by about one hour each day (Nicholls, 2019). Circadian desynchrony has been tied to numerous health consequences such as metabolic syndromes and mental health conditions (Potter, 2016; Stubblefield, 2016). Because of this, circadian disruption produced by misalignment of external time cues has become a health concern, and studies into the flexibility of these rhythms in alternative entrainment paradigms can shed light onto the most effective way to reduce this disruption. One such alternative entrainment schedule is known as bifurcation, a phenomenon where a unimodal pattern becomes a bimodal pattern, effectively splitting the 24 hour day into two (Gorman, 2003). Previous studies from our lab have explored bifurcation at the level of behavior, and discovered that previous bifurcation enables rapid re-entrainment of behavior following a 12 hour phase shift (Harrison, 2015). Additionally, we have also found that the addition of dim green light (lux <0.01) at night can help expand the established limits of entrainment to shortened T cycles for behavior as well (Walbeek, 2017). The present studies examine the effects of these two alternative entrainment paradigms at the molecular level in peripheral tissues.

In chapter 1, we explore how bifurcation of rhythms with the addition of dim green light can increase the resetting efficiency of locomotor and peripheral gene expression rhythms. Bifurcation is the phenomenon of inducing a bimodal rhythm through a split light dark cycle with two subjective days and nights (LDLD), or a waveform manipulation. An experimental paradigm of simple light manipulations allowed us to

induce jet lag in mice that have and have not been previously bifurcated and examine the differences in rhythm re-entrainment rates.

In chapter 2, we investigate the lower limits of hepatic clock gene expression flexibility. Current literature has established the limits of entrainment for liver clocks to be about 22-26 hours. These rhythms, however, are capable of phase advances and delays up to 6 hours, indicating the limit of entrainment may be wider than currently known. In order to answer this question, we housed mice in an 18 hour LD cycle with a 5 hour time restricted feeding window every 18 hours. If the liver is capable of a 6 hour phase advance, the implementation of 18 hour time cues should lead to stable entrainment of clock gene expression to T18. Chapter 1 represents a complete re-analysis of a dataset collected by Elizabeth Harrison, while chapter 2 was conducted in entirety by the author.

## Chapter 2: Bifurcation of the circadian waveform enables efficient resetting of clock gene rhythms following simulated time zone travel


### Abstract

Tight synchronization between body tissues and the external light dark schedule, mediated by the suprachiasmatic nuclei, is important in maintaining optimal health. Limited flexibility of these rhythms to change makes them susceptible to desynchrony when perturbed by a change in lighting schedule, posing a challenge to shift workers and those traveling between time zones. Recent findings have illuminated bifurcation as a way to potentially increase the resetting efficiency of these rhythms. To investigate whether bifurcation can aid in the resetting of circadian rhythms throughout the body, we stably entrained a subset of mice to bifurcated conditions and examined both activity and genes expression rhythms in peripheral tissues on the third day following a simulated jet lag scheme. Initial gene expression rhythms under bifurcated conditions revealed a reduced fit to a 24-hour sine curve due to a dampened amplitude. Robustness of the peripheral rhythms was rescued after the third day in new light conditions, and more closely matched the target phase and amplitude than the gene expression rhythms of previously unbifurcated tissues. Additionally, behavioral rhythms appeared to be fully reset in LDLD mice, but not in LD mice. Thus, we propose that bifurcation may increase the flexibility of both activity and peripheral rhythms in the body.

## Introduction

The existence of circadian rhythms within the body function to anticipate and entrain to daily fluctuations in the external environment, with synchronicity to the environment being largely mediated by a central oscillator, the suprachiasmatic nuclei (SCN), within the brain (Welsh, 2010). Cells themselves also contain an autonomous, self-sustained molecular clock that becomes aligned with the environment through numerous physiological cues stemming from the SCN, and are referred to as peripheral rhythms. Overall, the rhythms of the body are regulated hierarchically by a central oscillator, but exist at the cellular level (Rosenwasser, 2015). Because lighting information is received through the retino-hypothalamic tract and processed in the SCN, one's lighting schedule has the ability to not only influence sleep/activity cycles, but also internal peripheral rhythms. The introduction of an acute or chronic stimulus at the wrong time can lead to internal desynchrony, where an organism's rhythms are dampened due to dissociation of phase between individual clocks in a given tissue. (West) Artificial lighting and work schedules outside of the normal day have the potential to negatively impact health by inducing internal desynchrony (Nicholls, 2019).

Internal rhythms, while capable of shifting and resetting, are often slow to readjust to a large, acute change in the external environment. On average, rhythms adjust to a phase shift by about an hour each circadian cycle. Lack of rapid re-entrainment to new conditions poses an issue for internal synchrony and health, especially in those employed as shift workers (Nicholls, 2019). Bifurcation, enabled by introducing dim green light during the dark phase, is accomplished through splitting the photoperiod into two subjective nights and two subjective days (LDLD), which is

reflected as two functionally distinct and antiphase rhythms. Additionally, it is easily reversible (Gorman, 2003).

Research carried out by Watanabe et al. suggests that reorganization of clock gene expression in the SCN, which is the main light entrainable oscillator, may enable bimodal patterns in sleep/activity and physiological rhythms under bifurcated lighting conditions. Analysis of mPer1, mPer2, and mBmal1 gene expression in the ventrolateral-like (VM-L) and dorsomedial-like (DM-L) regions of the SCN revealed antiphase clock gene expression rhythms in the VM-L region compared to the DM-L region in mice steadily entrained to a bifurcated schedule (Watanabe, 2007; Harrison, 2015, Yan, 2010).

Reorganization of the circadian waveform, the shape of the 24 hour oscillation, temporally via bifurcation allows for a bimodal sleep/wake rhythm that may theoretically increase alertness during both day and night hours, as well as increase the flexibility of rhythm resetting (Harrison, 2016). Prior work done in Syrian hamsters indicates that previous bifurcation enhances rapid re-entrainment capabilities. Hamsters that were and were not initially bifurcated were challenged by 12 hour phase shifts, and those that had been previously bifurcated were capable of fully resetting locomotor rhythms within 3 days. In the non-bifurcated group; however, locomotor rhythms were still phase shifted by about 3.5 to 4 hours from their new time zone, illustrating the large acceleration of jet-lag recovery induced by bifurcation (Harrison, 2015). Here, we investigate whether rapid re-entrainment capabilities following jet lag extend to rhythms of peripheral tissues, as well. Using an experimental paradigm that aims to test parameters of

rhythmicity, we assess whether previous bifurcation is able to help peripheral rhythms reset more completely to new time zones within 3 days.

## METHODS

### Experimental Design

Both males and female C57BL/6 mice aged between 4-9 weeks were bred in-house from Jackson stock and used in approximately equal numbers (n=138; 24-30/group). One half of the animals in each group were placed on a reverse LD light/dark cycle for two weeks before baseline entrainment to facilitate later collection of tissues across multiple time points. Animals were then moved to individual cages equipped with running wheels near the time of lights off (8am or 8pm PST), where they remained in either LD 16:8 or LDLD 8:4:8:4 for two weeks. Of these stably entrained mice, three groups received significant changes to their lighting schedule to simulate jet lag. However, two groups of mice from the steady state baseline group did not receive further light manipulation and served as a control group. The three “traveling” groups were moved to either a Seattle time zone designation where lights went off at 8PM or a Moscow time zone where the lights went off at 8AM. One group from LD baseline conditions was moved to Moscow (LD Moscow; n=30), which represents a 12 hour shift from baseline entrainment. From LDLD baseline conditions, one group was moved to Moscow (LDLD Moscow; n=24) and another group was moved to Seattle (LDLD Seattle; n=24). All 5 groups remained in their respective lighting schedules for 3 days prior to tissue collection (Fig 2.1).

**Tissue Sampling & q-RT-PCR**

Kidney, liver, and lung samples were collected from 4-5 animals per traveling group every 4 hours across 24 h (24-30 total animals per experimental group) on the third day of the new LD schedule. Tissue samples were also collected from non-traveling controls in baseline LD and LDLD conditions with the same sampling paradigm on the same day tissue was collected from the shifting groups. Tissue was collected immediately following cervical dislocation, placed on dry ice, and stored at -80 C until processed. Tissues were homogenized and RNA purified using an RNEasy Mini Kit (Qiagen). cDNA was synthesized using the Super Script III First-Strand Synthesis System for RT- PCR (Invitrogen). qPCR was performed on a CFX384 Real-Time Detection System with SYBR Green (Bio-Rad) according to the manufacturer's instructions.

Raw mRNA expression levels were generated as an expression of the number of cycles required to reach the user-defined fluorescence level threshold of 500. Two determinations were made for each gene for each tissue sample. Where the difference between those determinations exceeded a value of 1 cycle, the determination that most closely represented the mean for that time point was included in the analysis (58/5796 determinations). Values were then normalized to expression levels for the same sample for the control gene Actb, using the formula (2(#ActCycles)/2(#ProbeCycles)) (Pfaffl, 2001). Data were averaged at each time point and the standard deviation was taken. No samples were excluded from analysis.

**Analysis of mRNA Expression levels/Statistics**

Least-squares sine curves were fit to the normalized expression profiles of six clock genes (Cry1, Cry2, Per1, Per2, Clock and Bmal1) in each of the three peripheral tissues for each experimental group using GraphPad Prism (Version 9.0.1, La Jolla, CA). Fits yielded by Prism were calculated by the following formula constrained to a 24 hour wavelength:

**Y= Amplitude*sin((2*pi*X/Wavelength)+PhaseShift) + Baseline**

Amplitude for each sine curve was calculated by subtracting baseline values from the highest point in the curve. Sine fits generated $R^2$ values, as well as estimated values and 95% confidence intervals for three parameters of interest: phase, amplitude, and baseline (mesor). Circadian rhythmicity of expression profiles was evaluated using the sum of squares value, $R^2$ value and the degrees of freedom for each series. Chi-square and binomial analyses were performed on the number of rhythmic genes in each group across all three tissues to test for systemic deviations in overall expression patterns. For all genes across groups, phase was derived from statistically significant sine fits, as a sine function is an appropriate fit for LD control data and we were interested in comparing deviations from this state caused by the re-entrainment paradigm across groups. Clock in the kidney was excluded from analysis because it was not significantly rhythmic under baseline LD conditions.

Extra-sums-of-squares F tests on fit curves allowed for intra-group comparisons. Extra-sums-of-squares F tests were conducted on the phases and amplitudes of sine fits for each gene in a given tissue that was rhythmic in both LD and the comparison group. For comparison of group differences, sine-fit-derived amplitude was calculated

as a percent of the LD control values in each gene for each tissue. In general, parametric tests were used to accommodate unequal variances across groups due to scaling or, in the case of phase comparisons, differences in sample size. Differences in amplitude and phase across groups were investigated using Kruskal-Wallis ANOVA with Wilcoxon signed-rank tests on paired comparisons. Initial phase differences under baseline lighting conditions were investigated using a Rayleigh test for uniformity. For a measure of phase in traveling groups relative to LD controls, we normalized the deviation in phase of the traveling groups to the target phase. The target phase was assigned the value of "0." LD controls were able to serve as targets for comparison because they did not undergo jetlag and reflect stable entrainment. Amplitude was also normalized relative to target. The amplitude of the target was given a value of "1," while the amplitude of the traveling group was divided by the phase of the target. Differences in total phase deviation following simulated jet lag were analyzed using a one way ANOVA with post-hoc Tukey's honestly significant difference between all groups. In all LD 16:8 conditions, including the Seattle and Moscow scotophases in the re-entrainment groups, lights off was designated as ZT12 (Johnson, Elliott, & Foster, 2003). For LDLD mice, the lights off that coincided with lights off in their prior LD schedule (8pm, "Seattle") was similarly designated as ZT12. All statistical tests described above and all plotted data pertain to minimum-normalized data as described previously, with one exception.

## RESULTS

**Rhythmicity is significantly different between clock gene expression in peripheral tissues in bifurcated and un-bifurcated mice.**

In order to establish differences in initial rhythmicity between peripheral tissues in mice that have and have not been bifurcated, we measured parameters of rhythmicity from 6 core clock genes from the kidney, liver, and lung. Male and female mice stably entrained to their respective LD (16:8) and LDLD (8:4:8:4) cycles for two weeks were sacrificed and tissue from the kidney, liver, and lung were collected for analysis. In total, 17 of 18 clock transcripts were rhythmic under LD conditions, excluding Clock in the kidney (Fig 2.2A). Clock in the kidney was therefore excluded from analysis because it is not possible to evaluate the degree of re-entrainment from a non-rhythmic pattern. All 18 transcripts were rhythmic under LDLD conditions (Fig 2.2B). Following bifurcation, 12 out of 18 total genes experienced a dampened amplitude (chi-squared test; p-val= 0.000091), while another 5 remained similar to the amplitude of LD conditions (Fig 2.3). These results suggest that bifurcation may dampen rhythmicity of certain clock genes in peripheral tissues.

In order to analyze the initial phase distribution of transcripts under two different lighting schedules, we utilized a Rayleigh test to compare relative phases. Because entrainment to LD and LDLD produces two different waveforms, we were not able to directly compare phases of the two conditions. Thus, we analyzed the dispersion of transcript phases in LDLD. Because clock gene expression follows a specific temporal pattern in stably entrained peripheral tissues, (Husse, 2014) phases were normalized relative to LD transcripts, which were assigned a value of “0.” Rayleigh test analysis revealed that bifurcated clock transcripts had a wide, unclustered phase distribution (Fig 2.2C; r= 0.51932519, df=16). These results suggest that the relative phase of clock transcripts in peripheral tissues is not preserved when mice are under bifurcated lighting

conditions. Thus, the lack of preservation of phase peripheral tissues in mice further suggests that rhythmicity is altered during bifurcation.

Goodness of fit was analyzed as a measure of how well these peripheral clock transcripts fit a sine curve. We took $R^2$ values from each clock gene sample under LD and LDLD conditions and compared them. Overall, 16 of 17 LDLD clock transcripts were quantitatively lower than LD clock transcripts (binomial test, $p < 0.001$). In the kidney, all clock transcripts were quantitatively different in their goodness of fit. Bmal1, Cry1, Cry2, Per1, and Per2 all had a decreased goodness of fit in relation to LD (Fig 2.4A). Clock, however, had a higher goodness of fit in LDLD than LD conditions in the kidney. Clock transcripts of the lung reflected the same trends in goodness of fit that were present in the kidney (Fig 2.4C). The liver, however, exhibited a decreased goodness of fit for all LDLD transcripts compared to LD clock transcripts (Fig 2.4B). The decrease in fit to a normal sine curve, with the transcripts being less sinusoidal, further indicates that rhythmicity between clock transcripts in bifurcated and un-bifurcation states is significantly different.

**Peripheral tissues that have undergone bifurcation reset to new time zones more quickly than unbifurcated peripheral tissues.**

In order to examine whether there were differences in resetting and whether those differences allowed for more efficient resetting following bifurcation, we compared parameters of rhythmicity following simulated jet lag. As described, three groups of mice that had been stably entrained to either LD or LDLD conditions underwent a simulated jet lag. Following stable entrainment to LD and LDLD conditions, a subset of mice from

each condition were moved to new time zones (Seattle and Moscow) for three days prior to tissue collection for clock gene analysis.

*Amplitude.* Tissue analysis 3 days after induced jetlag initially revealed that the transcripts generally followed a strong sinusoidal rhythm (SFig 2.1). We next explored how the clock gene amplitude differed between our traveling groups. For the group that was not bifurcated and experienced a 12 hour phase shift (LD Moscow), 9 of 17 transcripts were significantly different from the target amplitude, and of those 9, 8 transcripts had a quantitatively lower amplitude than the target. (Fig 2.5), suggesting that these transcripts had not been re-entrained. For the remaining 8 LD Moscow transcripts, we can consider them re-entrained to the target because the difference was not statistically significant. In LDLD Seattle mice, 14 of 17 peripheral clock transcripts were not significantly different in amplitude compared to target transcripts. In the 3 transcripts that were significantly different, the target amplitude was quantitatively higher than the LDLD Seattle transcript amplitudes for 2 of the samples (Fig 2.5). In LDLD Moscow mice, 12 out of 17 clock transcripts were not significantly different in amplitude compared to target amplitude. Of the 5 significantly different transcript amplitudes between the two groups, 3 LDLD Moscow transcripts had a quantitatively lower amplitude than the target (Fig 2.5). Between previously bifurcated and non-bifurcated groups, amplitude was significantly lower in the non-bifurcated groups (Chi-squared test, $p = 0.0357$), indicating that previous bifurcation leads to more efficient rhythm resetting. Many tissues that showed a dampened amplitude under initial bifurcated conditions had an increased amplitude following the simulated jetlag. These data reflect that previous bifurcation may aid in more efficient resetting, as both LDLD groups had a

greater portion of transcripts with amplitudes that were not significantly different from target amplitude.

*Phase*. In order to examine another parameter of rhythmicity, we also compared the phases of LD to Moscow transcripts, LDLD to Seattle, and LDLD to Moscow to target phases of control mice. A phase similar to the target phase indicates that the clock is almost or completely reset to the new time zone. Unbifurcated tissues jetlagged to Moscow had the least amount of clock transcripts in a similar phase to the target - with only 9 out of 18 being in a similar phase. The other 8 transcripts peaked later than the target phase (Fig 2.5). Bifurcated mice moved to the Seattle time zone also had 9 transcripts in a similar phase to the target. The other 8 transcripts, however, 6 of the genes peaked later, while 2 peaked earlier (Fig 2.5). In previously bifurcated mice moved to the Moscow time zone, 10 out of 17 clock genes were in a similar phase to the target, while the 4 transcripts peaked later and 3 transcripts peaked earlier (Fig 2.5).

The total phase deviation between all three groups in all three tissues was compared to determine efficiency of resetting between bifurcated and unbifurcated conditions. In all three tissues, the LDLD Moscow group had the quantitatively lowest total phase deviation (mean= -0.02528 hours) from the target, while the LD Moscow group had the quantitatively largest phase deviations (mean= 0.51665 hours). The LDLD Seattle group had a total phase deviation that was a quantitative intermediate (mean= 0.19101 hours) between LDLD Moscow and LDLD Seattle. Overall, groups with previous bifurcation showed a statistically significant difference in total phase deviation when compared with unbifurcated groups after 3 days in simulated jet lag conditions (Fig 2.6; p-val= 0.0162; One Way ANOVA). Intragroup comparisons show that the mean

phase deviation between LD Moscow and LDLD Moscow was significantly different (p-val= 0.0123; Tukey Kramer HSD), while the deviation between LDLD Moscow and LDLD Seattle was not significantly different (p-val= 0.4654; Tukey-Kramer HSD). However, the mean phase deviation LD Moscow and LDLD Seattle were also not significantly different either (p-val: 0.1836; Tukey-Kramer HSD). These results indicate that peripheral clock transcripts in previously bifurcated mice are able to reach their target phases more completely than peripheral clock transcripts in mice not previously bifurcated.

*Goodness of fit.* Additionally, goodness of fit was again measured to examine how well data fit a 24 hour sine curve. In 14 previously bifurcated clock transcripts, the goodness of fit for the data was similar or better than the goodness of fit for the unbifurcated Moscow tissue data (binomial test; p-val= 0.011673). Clock in the kidney and the lung were the only transcripts where goodness of fit was increased in the LD Moscow group and decreased in the LDLD groups (Fig 2.7A, C). In a bifurcated state, goodness of fit tended to be low (Fig 2.4). However, it seems that the movement to a new, unbifurcated time zone allows for the goodness of fit of clock transcripts of peripheral tissues to improve (Fig 2.7). This may be due to the size of the amplitude in either condition. The dampened amplitude under bifurcated conditions may lead to the low goodness of fit that we observed. Likewise, the increase in goodness of fit may be related to the rebound of amplitude following being moved to a new time zone. Future research is needed to explore the relationship between amplitude and goodness of fit. Overall, these results demonstrate a greater speed of resetting following bifurcation of peripheral tissues.

## DISCUSSION

Through a simulated jet lag paradigm, we were also able to analyze rhythmicity differences in peripheral tissues that indicate previous bifurcation in CB57BL/6 mice aids in more efficient resetting. Gene expression of clock transcripts in the kidney, liver, and lung under baseline LD 16:8 conditions was quite robust with a strong amplitude, a small distribution of peak phases, and a moderate to strong goodness of fit to a 24 hour sine curve. Clock gene expression under baseline bifurcated conditions in LDLD 8:4:8:4, however, exhibited differences in rhythmicity compared to clock gene expression under non-bifurcated conditions. LDLD clock gene transcripts had a dampened amplitude, wide peak phase distribution, and a low goodness of fit to a 24 hour sine curve. This suggests that peripheral clocks have been temporarily re-organized under bifurcated lighting conditions, which is consistent with findings from Watanbe et al. that describe antiphasic oscillations between two regions of the SCN (Watanbe, 2007). The dampened amplitude may be a result of the opposing signals from the VL-like and DM-like portions of the SCN.

Following the analysis of the rhythmicity of clock transcripts under baseline lighting conditions, we introduced mice to a simulated 12 hour jet lag paradigm and investigated peripheral clock gene rhythms 3 days after initial “traveling.” Clock transcripts from mice from the unbifurcated state jetlagged by 12 hours to the Moscow time zone exhibited a dampened amplitude, wider phase distribution, and a decreased goodness of fit to a 24 hour sine curve in comparison to baseline LD conditions. Dampening of clock rhythms is typical of jetlagged tissues (Kori, 2017). The LD Moscow group also had the largest total phase deviation from the target, indicating that

unbifurcated tissues had not completely re-entrained to their new lighting conditions by 3 days. In previously bifurcated mice, peripheral clock transcripts from both the Seattle and Moscow time zones showed a rebound in amplitude, a reduced relative phase distribution, and an increased goodness of fit to a 24 hour sine curve compared to LDLD baseline conditions. Additionally, the LDLD Moscow transcripts had the lowest total phase deviation from the target phase - while LDLD Seattle transcripts' total phase deviation fell between LDLD Moscow and LD Moscow. LDLD Moscow transcripts' phase deviation was significantly different from that of LD Moscow, and was not significantly different from LDLD Seattle. These results indicate that peripheral tissues in both LDLD Seattle and LDLD Moscow were more completely reset after 3 days than the previously unbifurcated group. Interestingly, total phase deviation between LD Moscow and LDLD Seattle was not significantly different.

The current study extends the finding of increased resetting efficiency of behavioral rhythms in previously bifurcated hamsters (Harrison, 2015). Unpublished data from our lab shows that, through a simulated jet lag paradigm, re-entrainment of activity rhythms of previously bifurcated mice was complete after 3 days in a new light dark environment. Behavior was analyzed following one day in jet lagged conditions, and the variable phase dispersion of activity between LDLD Moscow and LDLD Seattle groups indicated incomplete resetting. On the third day, however, peak activity between LDLD Moscow and LDLD Seattle was antiphase from each other, which is indicative of the activity rhythms in either group being fully reset to their new respective lighting conditions.

Together, these results indicate that previous bifurcation aids in resetting efficiency of peripheral tissues that have experienced jetlag. Three days after we simulated jet lag, mice that had been previously bifurcated appeared to reset more completely in this time frame. Future research is needed to investigate the mechanism by which bifurcation leads to quicker resetting of peripheral tissues, but we hypothesize that the initial dampening of the clock under bifurcated conditions might provide the proper molecular landscape needed to reset at an increased pace (Noguchi, 2020). This discovery may be of importance to the health of shift workers around the globe, as many shift workers suffer from circadian disruption-related diseases such as depression, cardiovascular disease, and metabolic disease. Bifurcation may be able to serve as a future tool to reduce the circadian disruption associated with frequent scheduling changes and overnight shifts (Walbeek, 2017).

Chapter 2, in part is currently being prepared for submission for publication of the material. Harrison, Elizabeth; Koretoff, Alexandra. The thesis author was the primary researcher and author of this material.

## FIGURES

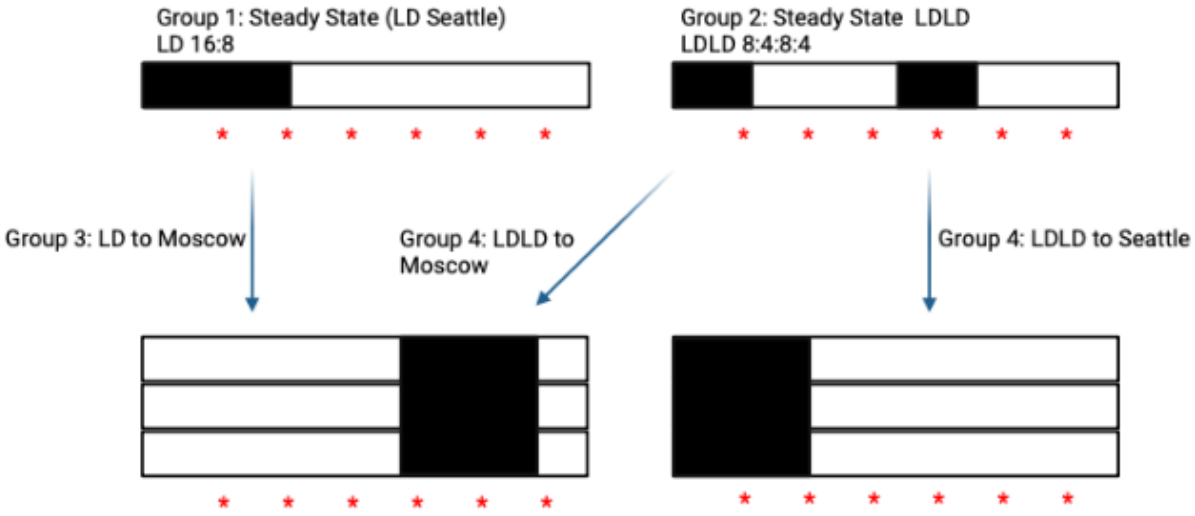


**Figure 2.1: Simulated Jet Lag Paradigm**
General experimental paradigms made with BioRender. Mice stably entrained to steady state conditions (LD or LDLD) had tissues collected every 4 hours for 24 hours, noted by red asterisks. Groups of mice from each steady state group were chosen to undergo a 12 hour time zone shift (blue arrows), and tissues were collected every 4 hours for 24 hours after 3 days in their new time zone. For ease of the reader, time zone shifts are referred to by “Seattle” (lights off at ZT8) or “Moscow” (lights off at ZT20).

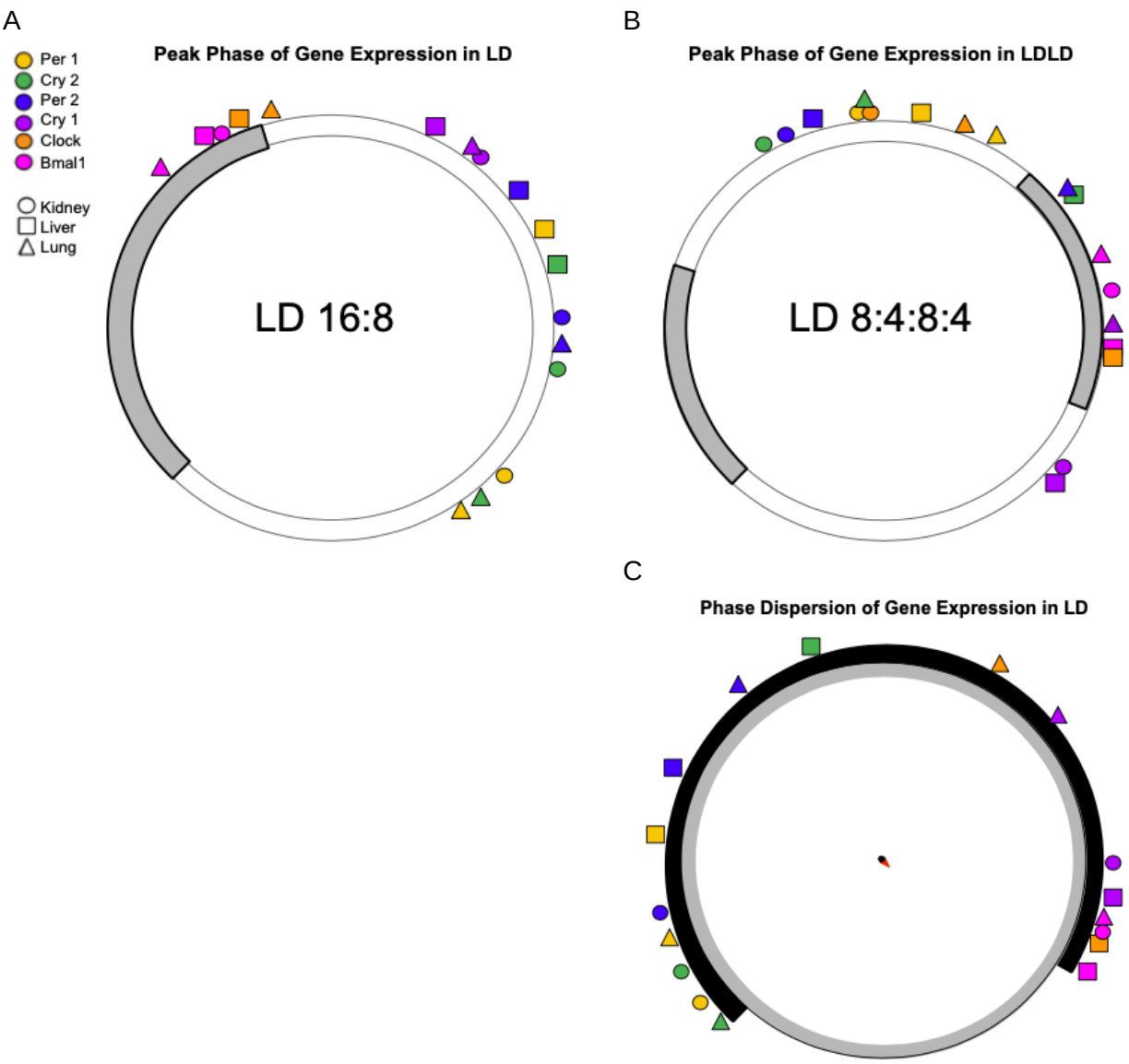


**Figure 2.2: Visual Representation of Peak Phases and Total Phase Dispersion of Clock Gene Transcription by Tissue and Total Relative Phase Deviation in Baseline Conditions**

(a) Polar plots depict the peak phase of each gene in each tissue from the baseline, which was determined by sine fitting in GraphPad Prism Version 9. Phase is plotted by zeitgeber time (ZT) and is represented as angular coordinates. (a) Peak phases of clock transcripts in LD conditions. Clock from the kidney was excluded from analysis. (b) Peak phases of clock transcripts in LDLD conditions. (c) Polar plot depicting phase dispersion for all 17 genes, excluding Clock in the kidney, in LDLD conditions relative to their time of peak expression in LD. Phase of all 18 genes was analyzed via Rayleigh testing (critical r> 0.4, df=16). The mean vector is depicted as a small red arrow (X= 0.04715718, Y= -0.0217529), while the phase distribution of all genes for LDLD is noted by a black arc. Each clock gene is color coded while the corresponding tissue that the gene was isolated from is denoted by shape. Dark phase of the lighting schedule is indicated by grey shading in part (a) and (b). All animals in the dark phase received dim light (<0.01 lux). Distances of colored shapes from the circle are only for viewing ease of different transcripts, but have no meaning.

A

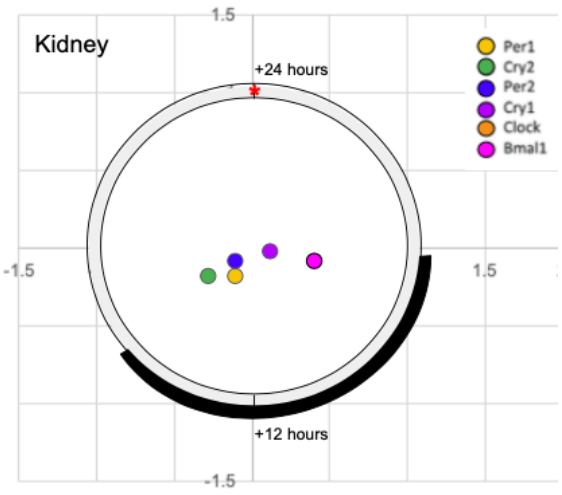


B

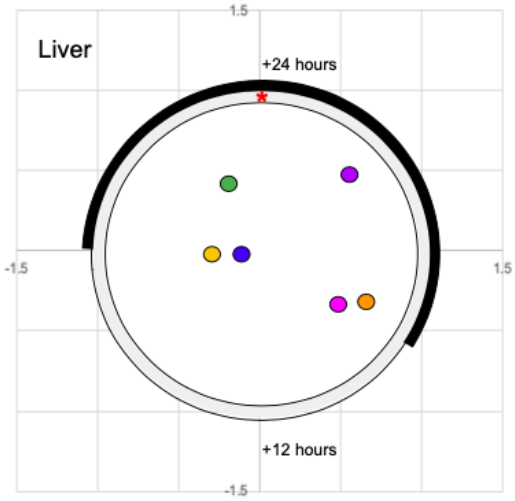


C

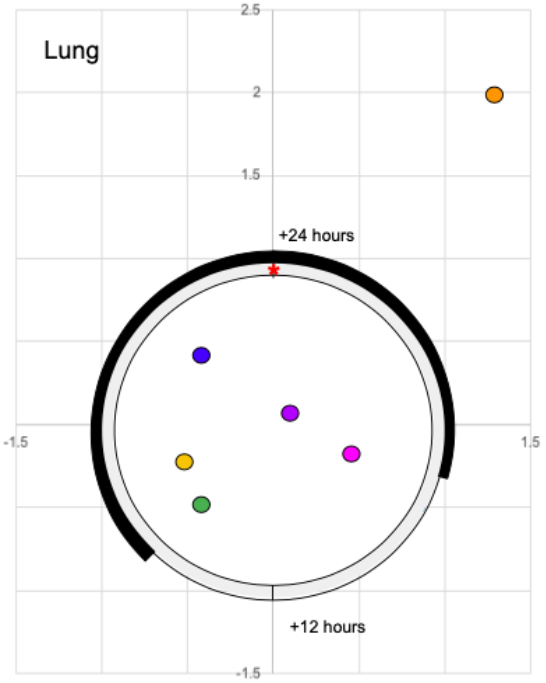


**Figure 2.3: Phase and Amplitude of LDLD Relative to LD in Baseline Conditions**
Radial plots depicting the phase and amplitude of baseline LDLD clock transcripts for (a) the kidney, (b) the liver, and (c) the lung normalized to LD clock transcript phase and amplitude. The light circle represents the amplitude of LD transcripts. Black curves around the circle indicate the phase distribution of LDLD genes. Distance from the circle represents the amplitude of LDLD transcripts in each tissue relative to the LD amplitude of the respective tissue. Clock was excluded from analysis in the kidney, as it was not rhythmic under LD conditions.

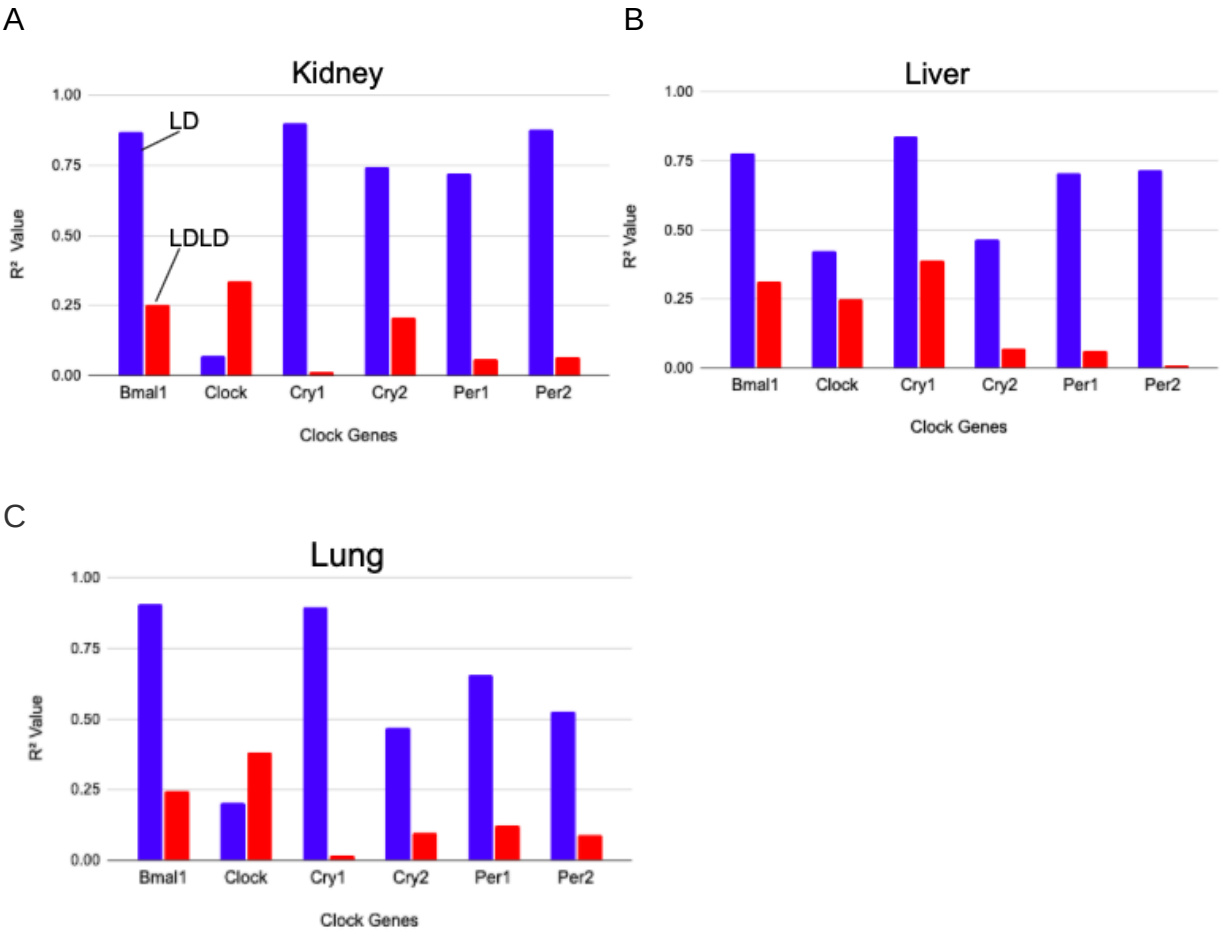


**Figure 2.4: Goodness of Fit for LD and LDLD Clock Genes at Baseline**
Column graphs depict the goodness of fit of clock gene expression at baseline to sine curves for each gene in three sampled tissues: (a) kidney, (b) liver, and (c) lung. Goodness of fit for each gene was acquired from GraphPad Prism. Goodness of fit in LD conditions is noted in blue while goodness of fit for LDLD conditions is noted in red. Goodness of fit was lower in LDLD in all transcripts with the exception of Clock in the kidney and lung.

**Figure 2.5: Radial Plots of Relative Phase and Relative Amplitude to Stably Entrained Controls Following Simulated Jet-Lag**

Radial plots depicting the phase and amplitude post-jet-lag of (a) kidney, (b) liver, and (c) lung clock transcripts normalized to LD clock transcript phase and amplitude, as stated previously. The grey circle represents the target amplitude of a stably entrained control. Red asterisks at the top of each circle represent the target phase. Clustered, colored circles refer to transcripts from their respective tissue. The black shaded region along the circle represents the phase distribution of jetlagged transcripts relative to the phase of stably entrained targets. Previously bifurcated transcripts generally had a lower phase distribution compared to the target, indicating a preservation of phase and a higher resetting efficiency.

**A**

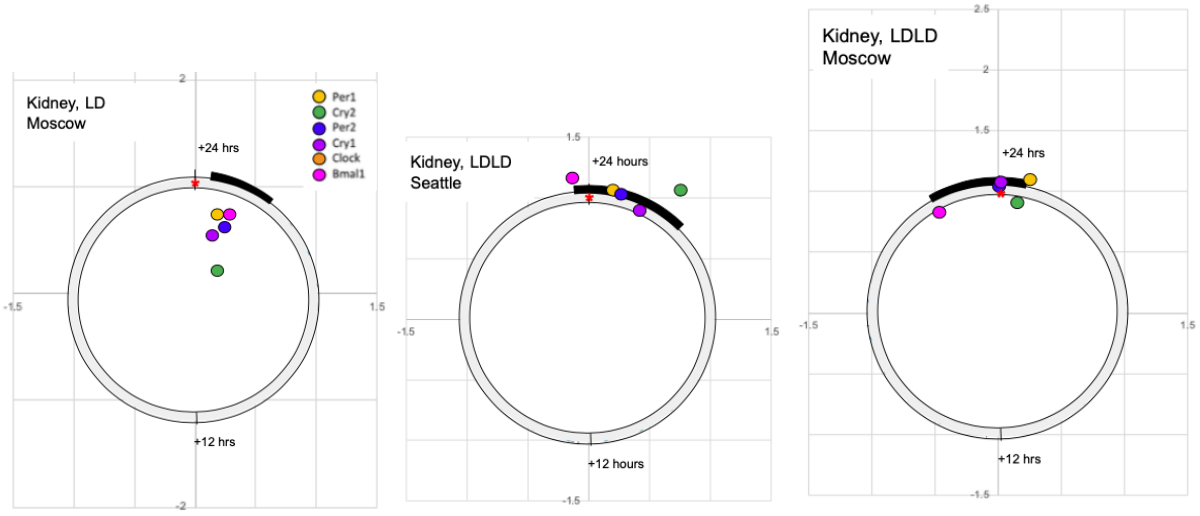
Kidney, LD
Moscow
Per1
Cry2
Per2
Cry1
Clock
Bmal1
+24 hrs
+12 hrs
Kidney, LDLD
Seattle
+24 hours
+12 hours
Kidney, LDLD
Moscow
+24 hrs
+12 hrs

**B**

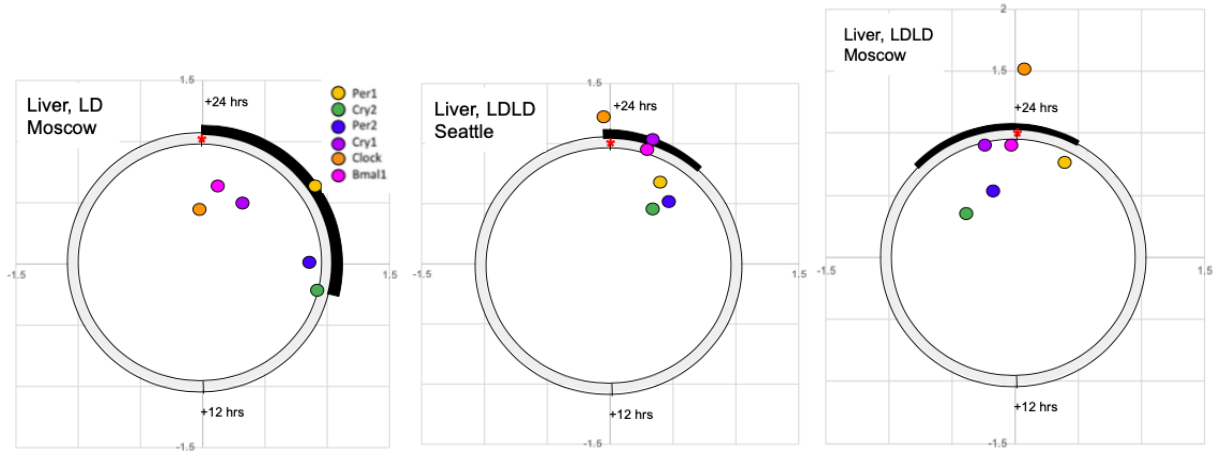
Liver, LD
Moscow
Per1
Cry2
Per2
Cry1
Clock
Bmal1
+24 hrs
+12 hrs
Liver, LDLD
Seattle
+24 hrs
+12 hrs
Liver, LDLD
Moscow
+24 hrs
+12 hrs

**C**

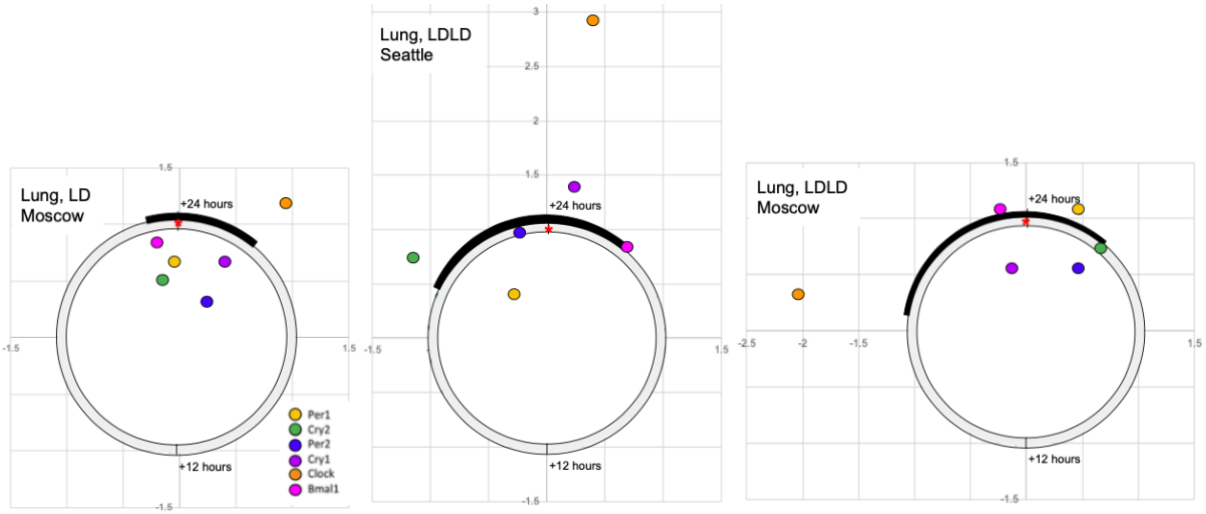
Lung, LD
Moscow
+24 hours
+12 hours
Per1
Cry2
Per2
Cry1
Clock
Bmal1
Lung, LDLD
Seattle
+24 hours
+12 hours
Lung, LDLD
Moscow
+24 hours
+12 hours

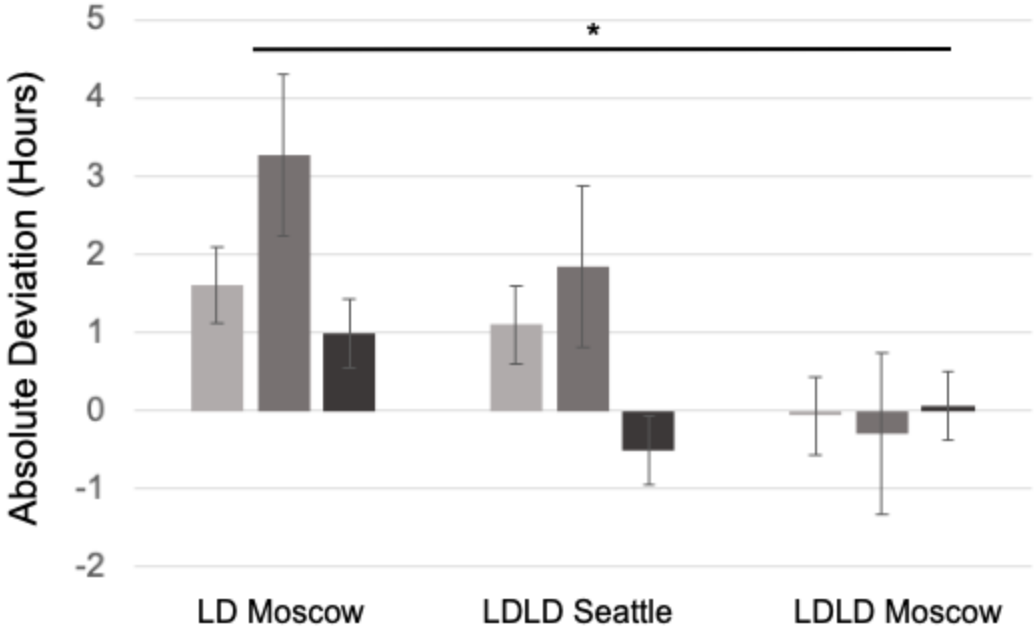


**Figure 2.6: Absolute Deviation in Phase from Target Following Simulated Jet Lag**
Column plot depicting the total deviation in phase from target. Following phase normalization, total deviation in phase was converted from radians to hour angles. Mean and standard deviation were calculated from hour angles and used for analysis via one way ANOVA with post-hoc Tukey HSD test (*p-value < 0.05). Grey-scale bars correspond to tissue type in which transcripts were sampled, with the lightest representing the kidney, intermediate representing the liver, and darkest representing the lung. Clock transcripts in the kidney were excluded from analysis, as Clock was not rhythmic in baseline LD conditions in the kidney. Data presented as mean +/-s.e.m. The total phase deviation from the target in LDLD Moscow was significantly lower than the LD Moscow group, indicating more complete resetting of peripheral gene expression rhythms following bifurcation.

**Figure 2.7: Goodness of Fit for Clock Gene Expression**
Overlaid bar graphs displaying the change in goodness of fit from baseline to 3 days post-simulated jet lag. $R^2$ values for each clock gene in the (a) kidney, (b) liver, and (c) lung were gathered from GraphPad Prism. Goodness of fit indicates how well the transcripts of a given gene fit a sine curve. Sine curves were generated via GraphPad Prism and were constrained to transcripts that had only a 24 hour period. Black bars indicate the goodness of fit at baseline conditions (LD or LDLD) and arrows represent what the goodness of fit value was after 3 days in their respective simulated jet lag conditions. Red shading indicates a decrease in goodness of fit from baseline following jet let. Blue shading indicates an increase in goodness from baseline. In general, previously non-bifurcated tissues experienced a decrease in the goodness of fit to the sine curve, while previously bifurcated tissues experienced an increase in the goodness of fit.

A

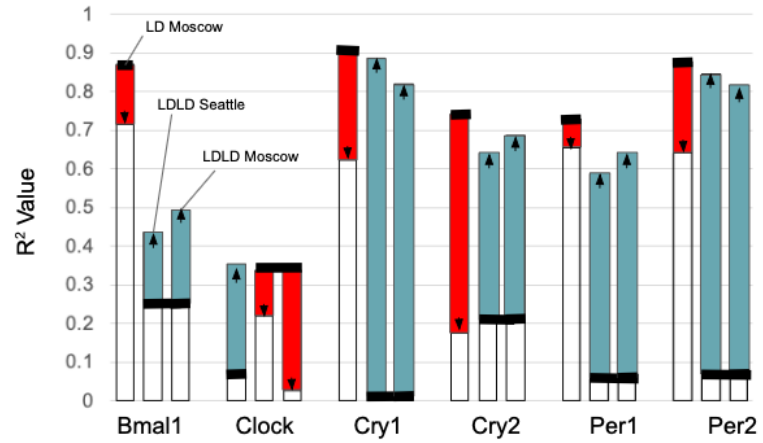
LD Moscow
LDLD Seattle
LDLD Moscow
R² Value
1
0.9
0.8
0.7
0.6
0.5
0.4
0.3
0.2
0.1
0
Bmal1
Clock
Cry1
Cry2
Per1
Per2

B

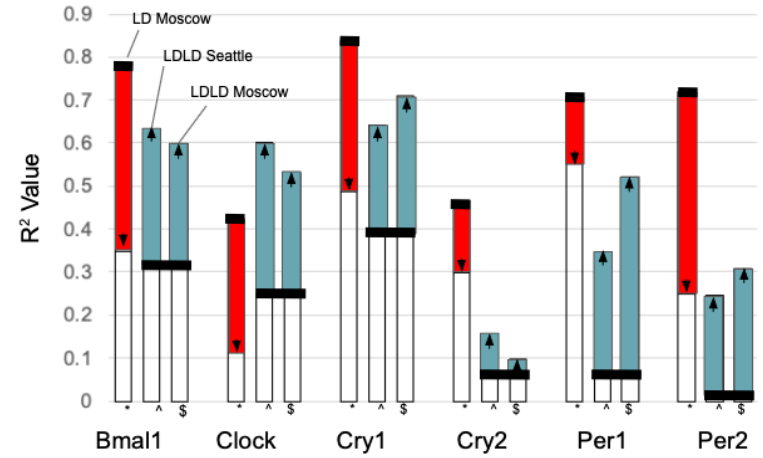
LD Moscow
LDLD Seattle
LDLD Moscow
R² Value
0.9
0.8
0.7
0.6
0.5
0.4
0.3
0.2
0.1
0
* ^ $
Bmal1
Clock
Cry1
Cry2
Per1
Per2

C

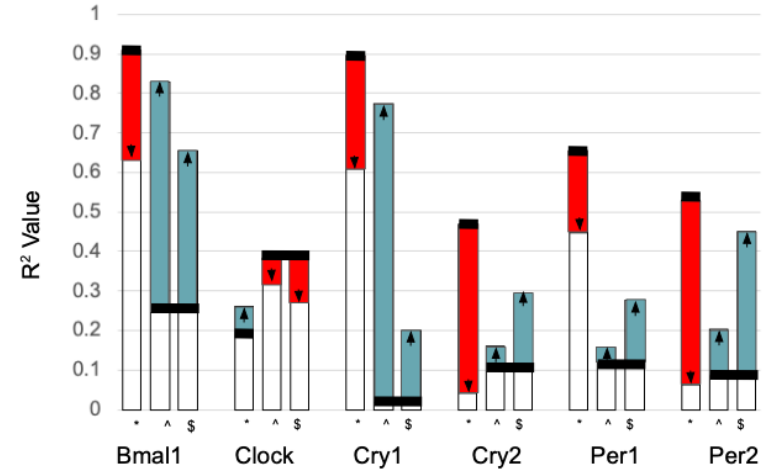
R² Value
1
0.9
0.8
0.7
0.6
0.5
0.4
0.3
0.2
0.1
0
* ^ $
Bmal1
Clock
Cry1
Cry2
Per1
Per2

***SI INFO***

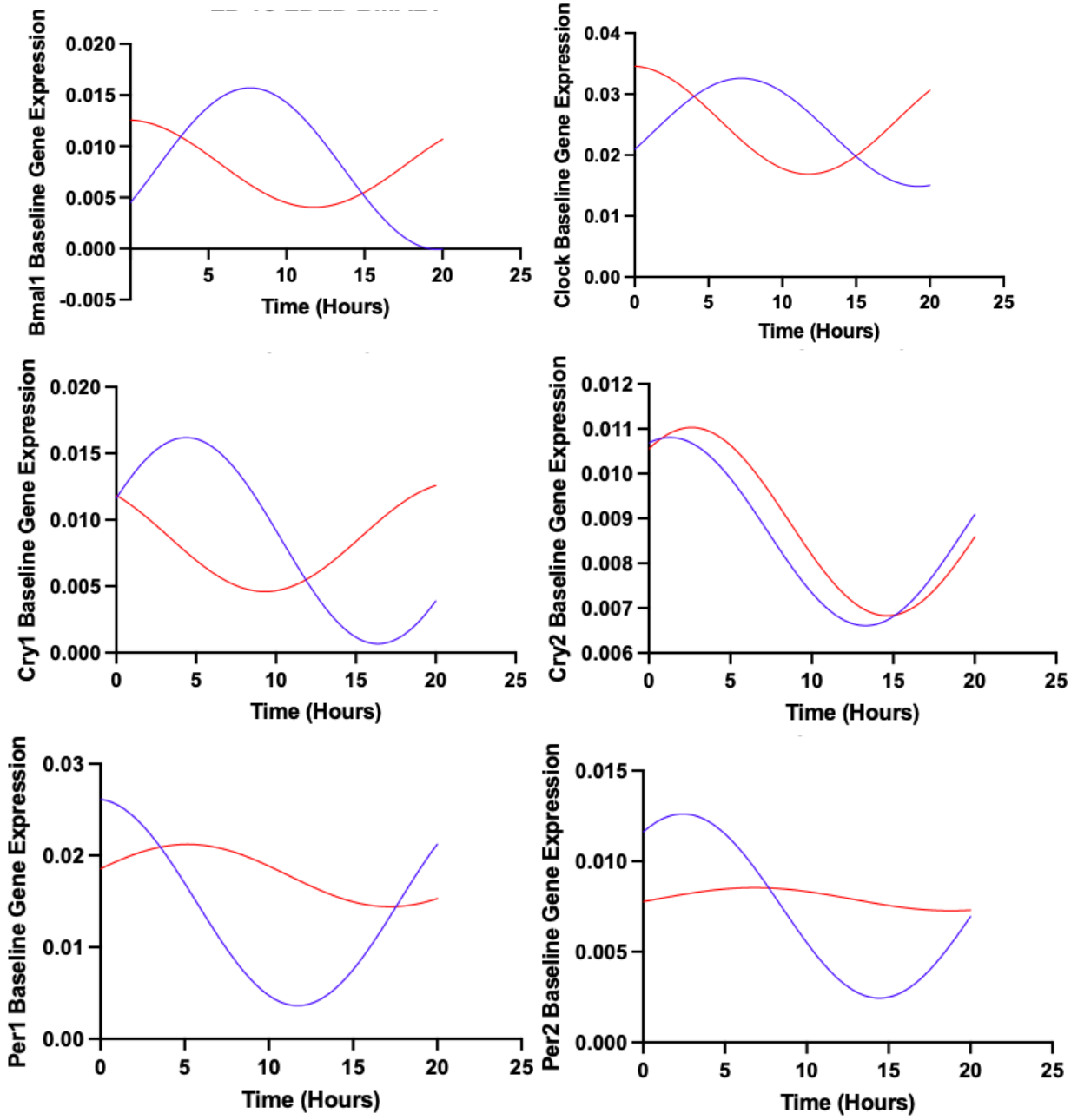


**Supplemental Figure 1: Sine Curves for LD vs. LDLD Data**

Clock gene expression data for 6 clock genes (Cry1/2, Per1/2, Bmal1, and Cry1) at baseline in LD (blue) or LDLD (red). Sine fits were generated through a least-squares linear regression analysis in GraphPad Prism. In general, the amplitude of sine curves matching LDLD were dampened.

## Chapter 3: Hepatic clock gene expression cycles with 18 hour periodicity when put on T18 lighting and feeding schedule


### ABSTRACT

Hepatic circadian rhythms cycle on a near 24 hour basis and exist to anticipate nutrients and regulate metabolic processes. A lack of alignment between the hepatic rhythms and the external environment has been shown to lead to metabolic dysfunction and health complications, and is considered circadian disruption. As a result, there has been growing interest in understanding the limits and mechanisms that underlie circadian flexibility. Here, we investigate whether an 18 hour day is within the limits of entrainment for hepatic clock genes by housing mice in LD13:5 and restricting food availability to the 5 hour dark window. When an 18 hour signal was reinforced via light and nutrient stimuli, murine hepatic clock gene expression cycled with a low amplitude and near 18 hour periodicity. These results suggest that the molecular clocks of peripheral tissues have a wider range of entrainment than previously understood, and that the dampening of rhythms enables extraordinary flexibility.


### INTRODUCTION

Circadian rhythms are generated by complex, cell-autonomous time-keeping systems within the body and consist of the central oscillators and the individual clocks that exist within peripheral cells. These clocks run on a near 24 hour loop that is driven by a transcription-translation feedback loop involving the core clock proteins PER, CRY, BMAL1, and CLOCK (Tahara, 2016. Trott, 2018). Additionally, this feedback loop's

robust rhythm is stabilized by a secondary loop involving BMAL1, RORα, and REV-ERBα and β. Within the context of the liver, circadian rhythms are important for maintaining liver homeostasis as well as anticipating the daily rhythms in nutrient availability (Tahara, 2016). Because maintenance of homeostasis and anticipation of metabolic needs are extremely important relative to metabolic health, synchronization of environmental stimuli and the endogenous hepatic clock allows for optimal health outcomes. Desynchronization between the environment and the hepatic clock has been shown previously to lead to metabolic dysfunction and eventually diseases, such as obesity, hyperlipidemia, cancer, and cardiovascular disease (Chaix, 2016). While light has a potent synchronizing effect on peripheral clocks, research has recently moved toward studying the effects of daily feeding and fasting patterns on the hepatic clock (Carneiro, 2012).

There are a range of non-photic stimuli capable of influencing peripheral circadian rhythms. Patterns of daily nutrient-intake serve as one such powerful, non-photic zeitgeber. Food entrainment occurs independently of the light-dark cycle through a separate, self-sustained oscillator, and peripheral tissues are capable of entraining to nutrient availability to differing degrees. Little about location of the food entrainable oscillator (FEO) is currently known, but food availability is capable of uncoupling peripheral rhythms from the master photic synchronizer, the suprachiasmatic nuclei (SCN), and entraining them to cycles in nutrient availability (Carneiro, 2012). Typically, mice consume the bulk of their food during the dark phase, as they are nocturnal, and exhibit foraging-related wheel running. When put into constant light conditions or unable to perceive light, their feeding rhythm free runs, indicating that food is a powerful

zeitgeber and not simply the result of masking of LD-related rhythms (Boulos, 1980). Additionally, when food is restricted to the light phase, mice begin to run on their wheels during the day in anticipation of their meal, and wheel running activity during the dark is attenuated (Mistlberger, 1990, Rosenwasser, 1984). Food availability resets the hepatic clock by both directly influencing core clock genes and by modulating rhythmic gene transcription of feeding responsive transcripts (food induced and food repressed). The core hepatic clock itself is modulated by feeding stimuli through the differential response to insulin by PER1 and PER2, the former being suppressed by insulin and the latter being induced. Changes in the level of PER1 and PER2 in the cell result in an alteration in the levels of other core clock proteins (Tao, 2015), which illustrates the ability of nutritional availability to directly set the phase and amplitude of the hepatic clock (Vollmers, 2009).

Synchronization of biological rhythms to an environmental cycle less than 24 hours have been described previously. Entrainment to rhythmic external stimuli has its limits. The range of entrainment for a particular tissue is predicted by the magnitude of the largest phase advance (shortest period) and phase delay (longest period). In general, the in vivo range of entrainment for the hepatic clock has been established as T=22-26 hours (Hamaguchi, 2015), but phase advances of hepatic rhythms up to 6 hours have been generated with insulin administration (Yamajuku, 2012). The range of entrainment established by Hamaguchi et al., however, may not represent the full range of entrainment that the liver is capable of achieving. In their study, mice were kept on an 18 hour time-restricted feeding paradigm and in LD12:12, thus receiving both 18 and 24 hour cues at the same time, before PER2:luc rhythms were assessed in individual mice.

Rhythmicity of additional clock genes was not assessed. The 24 hour rhythmicity of the light:dark cycle may have interfered with hepatic entrainment to T18, as light is one of the most powerful zeitgebers.

Previous studies from our lab show that mice exposed to an LD13:5 cycle along with supplemental dim green light exposure (lux) were successful at entraining their activity rhythms to the 18 hour light dark schedule. Clock gene expression rhythms of the liver, however, continued to cycle on a near 24 hour basis (Walbeek, 2017). While exposed to a T18 light cycle, these mice were fed ad libitum, which likely uncoupled the liver clock from the main regulator of photoperiodic information - the SCN. The hepatic time keeping system possibly continued to follow the natural near 24 hour ad libitum feeding rhythm seen in mice (Walbeek, 2017). Feeding patterns during this study were not measured, and the necessity of an 18 hour nutrient signal remains open-ended. Thus, the current study aims to investigate whether an 18 hour rhythm is within the in vivo limits of entrainment of the murine liver with the addition of 18 hour light and food cues, and potentially broaden our understanding of circadian plasticity. Considering the role of the liver in energy homeostasis, it is conceivable that the hepatic clock plasticity to short days may be reinforced by a time restricted feeding regime occurring on an 18 hour basis. Utilizing an automated feeding apparatus to restrict mice to feeding during the 5 hour dark phase, we sought to see if the additional 18 hour time signal in food availability would enable hepatic clock gene expression to entrain to the shortened T cycle.

# METHODS

## Animals and Housing

Male CB57BL6 mice were housed in plastic cages without running wheels in well-ventilated environmental chambers and bred from male and female mouse pairs from Jackson Laboratories (Bar Harbor, ME). Chambers fit up to 16 cages and the temperature was continuously monitored. All colony mice were kept in a LD14:10 light cycle at the time of weaning (~6 weeks), and had ad libitum access to food (Purina, BioServ, San Diego, CA) and water. Colony mice were housed in a group of 3-4 mice, and were then moved to individual plastic cages (11.45”x7.0”) equipped with a running wheel at the start of the study. The environmental chambers were equipped with fluorescent lamps (lux=100-300) and additional dim green light (lux<0.01). At the start of TRF, mice were moved into a chamber with plastic cages (12.4”x5.5”) with running wheels that were compatible with an automated feeding system (Phenome Technologies, Skokie, IL). All experimental protocols were pre-approved and followed guidelines set by UCSD’s Institutional Animal Care and Use Program.

## Entrainment

64 male mice from the colony were moved from group housing to single housing in LD 14:10, fed ad libitum and received dim green light (lux<0.01). These mice remained in these conditions for an acclimation period of 3 weeks. Wheel running activity was monitored to confirm entrainment to T24. After 3 weeks of entrainment to T24, these mice (n=64) were switched to a T18 schedule (LD13:5) for two weeks with ad libitum feeding, and locomotor entrainment to the lighting schedule was assessed. In

all phases of the experiment, locomotor entrainment was measured by Vital View (Indian Harbor Beach, FL) as the number of half wheel revolutions within 6 minute bins. Mice who successfully entrained to T18 (n=46) were selected from the group and moved to a T18 time restricted feeding schedule in automated feeder cages. Food was made available to the mice only during the 5 hour dark period (ZT13-ZT18). Entrainment quotient (EQ) values, which quantify the strength of behavioral entrainment to T18, were calculated by taking the amplitude of wheel running with an 18 hour periodicity divided by the sum of amplitudes with T18 periodicity and T22-26 hour periodicity. The range of entrainment spanned from EQ=0.25-1.0, with the average EQ value being 0.727. Mice undergoing food restriction were weighed prior to treatment and again at the time of euthanasia. No statistical differences were found between the weights of mice following time restricted feeding, and the mice did not experience a significant change in body weight (>10% of body weight). Feeding activity was assessed with ClockLab Chamber Control (Actimetrics, Wilmette, IL).

**Tissue Collection/RNA Isolation**

After two weeks in TRF conditions, mice were sacrificed in groups (n=2) every 3 hours for 36 hours (ZT0.5-ZT33.5). Euthanasia was performed by CO2 chamber and cervical dislocation as a secondary method of death. For mice euthanized during the dark phase, dim red light was used. The bottom left lobe of the liver was collected immediately after death, stored in 1mL trizol, and placed into a -80℃. All tissues were collected within 30 minutes of the predetermined time of death. Liver samples were homogenized, and a phenol-chloroform extraction was then utilized to isolate RNA from

each liver sample, followed by treatment with Qiagen Minikit (Qiagen, Venlo, Netherlands) to purify the RNA. Additionally, all samples were subjected to treatment with Zymo Clean & Concentrate (Zymo Research, Irvine, CA, USA) to further purify DNA and concentrate the samples.

**RT-qPCR**

Using iScript (Bio-Rad, Hercules, CA, USA), 100 ng/uL cDNA was synthesized according to the manufacturer instructions and diluted 1:1. iQ SYBR Green (Bio-Rad, Hercules, CA, USA) was then added to each cDNA sample to make a 10uL reaction run on a CFX Connect Real-Time PCR Detection System (Bio-Rad, Hercules, CA, USA). Quantification cycles (Cq) were assessed by setting the relative fluorescence threshold to 100. Cq values for each sample were averaged for each qPCR reaction in a triplicate set, and the standard deviation between triplicate values was assessed. For triplicates with a standard deviation higher than 0.5, the outlier was excluded from the calculation of the average for that triplicate value. Average Cq values were then used to analyze gene expression relative to expression of housekeeping genes H2afz and Mapk3 with the ΔΔCT method (Livak, 2001, Pfaffl, 2001). Fold change was then calculated. PCR efficiency for each primer was approximately 1.1-1.45. 7 samples were excluded from overall analysis: 3 for low DNA yield and 4 that had to be moved to ad libitum feeding during the TRF phase. All primers were obtained from Integrated DNA Technologies (Coralville, IA).

Table 3.1: Primer Sequences

| ***Gene*** | ***Forward*** | ***Reverse*** |
|---|---|---|
| Bmal1 | tggaaccctaggccttcatt | ttcgatccagtgtgggagat |
| Clock | cttcctggtaacgcgagaaag | gtcgaatctcactagcatctgac |
| Cry1 | cactggttccgaaagggactc | ctgaagcaaaaatcgccacct |
| Cry2 | gcgtctgtttgtagtccggg | tcccaaagggttcagagtcata |
| H2afz | tcaccgcagaggtacttgag | gatgtgtggtggtgggatgacacca |
| Mapk3 | tccgccatgagaatgttataggc | ggtggtgttgataagcagattgg |
| Per1 | tgaagcaagaccgggagag | cacacacgccgtcacatc |
| Per2 | cttggggagaagtccacgta | tactgggactagcggctcc |

**Statistical Analysis**

Clock gene expression profiles (Cry1, Cry2, Per1, Per2, Bmal1, and Clock) normalized to H2afz and Makp3 were fit to 18 and 24 hour sine curves using a least-squares regression in GraphPad Prism (Version 9.3.1, La Jolla, CA). Curve fitting in Prism was set to compare which sine curve was a better fit via an Extra sum-of-squares F test, constrained to an 18 or 24 hour wavelength. For each sine curve, Prism calculated $R^2$ values as well as estimated values and 95% confidence intervals for the phase and amplitude of each gene. Rhythmicity of each gene was assessed using the $R^2$ values for each gene. Correlation coefficients between different gene pairs were calculated and statistical significance of correlations was determined by a two-tailed T test. To determine whether the phase under a T18 or T24 analysis accurately reflected proper gene expression patterns, phase information generated by prism was normalized to a “reference phase” from T24 control animals, which was assigned a value of “0.” Animals entrained to T24 were used as a reference to establish a normal clock gene expression phase relationship under stable entrainment. A paired T-test was utilized to evaluate the difference in goodness of fit to either a T18 or T24 sine curve.

# RESULTS

## Mice exposed to a T18 light schedule are capable of behavioral entrainment

In order to assess initial entrainment to the imposed cycles, wheel running data and ad libitum feeding rhythms were examined. Figure 3.1 outlines the general entrainment paradigm followed throughout the experiment and provides visual representation of locomotor entrainment quality for each experimental phase. Mice housed in the pre-treatment phase (LD 14:10, ad lib feeding, n=64), were well entrained to the 24 hour cycle as expected (Figure 3.1). These mice were then subjected to a shift to an LD13:5 light cycle, and entrainment was reassessed. Of these mice, the 46 best with the best entrained locomotor activity to T18 were moved into automated feeder cages and fed ad libitum while adjusting to the change in the physical environment. Following the adjustment period, food was restricted to a 5 hour window during the dark portion of the light cycle. Activity entrainment to T18 under a TRF was assessed by EQ values, with an EQ value of 1 representing full entrainment and a value of 0 representing a complete lack of entrainment. Locomotor entrainment status to T18 was variable. 22 of the 46 mice became well entrained to an 18 hour day, having both a strong peak at 18 hours on a periodogram and a majority of their activity line up with the dark cycle (Fig 3.1A). The other 24 mice had broad periodogram peaks between 22-26 hours, smaller 18 hour periodogram peaks, and a larger portion of activity occurring during the light phase (Fig 3.1B) The average locomotor EQ value of all mice was 0.727, with a standard deviation of 0.196. In general, the number of wheel revolutions after initiation of TRF decreased as a whole, which may be due to a change in the running wheel as dictated by the design of the automated feeder system. Overall, these

results meet the minimal expectations of and confirm the possibility of behavioral entrainment to T18, but activity entrainment was not as strong as our lab has previously seen (Walbeek, 2017).

The automated feeding system also allowed us to assess patterns in feeding entertainment. Each time a pellet was taken, it was automatically logged. Actograms of ad libitum feeding data show pellets being taken throughout the day, and there is no evidence of an 18 hour pattern in feeding behavior (SFig 3.1). This suggests that without the addition of a TRF, feeding rhythms do not entrain to T18. When food restriction was initiated, food was distributed throughout the dark phase, and food pellets dispensed by the automated feeder were rarely available outside of the feeding window (SFig 3.1). This suggests that time restricted eating was extremely effective in generating an 18 hour feeding behavior pattern, but cannot be called entertainment due to the fact that food restriction was manually imposed. These behavioral data, as a whole, indicate a wide range of entrainment that includes an 18 hour day.

**Hepatic clock gene expression rhythmicity entrains to LD13:5 after time restricted eating**

Because we observed successful behavioral entrainment to T18, we wanted to assess whether peripheral rhythms were cycling with 18 hour rhythmicity. Liver tissue collected after two weeks in T18 on a TRF was investigated via RT-qPCR. Rhythmic signal determinations were based on the goodness of fit to an 18 hour or 24 hour sine curve, the relationship among clock genes relative to each other, and the peak phase of each gene relative to peak phasing in 24 hour controls. 24 hours was chosen for the

comparison because free-running gene expression rhythms cycle on a near 24 hour basis, and inability to entrain to T18 would result in free-running. For each gene, goodness of fit to any sine curve was relatively low in general, but stronger for an 18 hour sine curve. Goodness of fit values to a T18 curve were on average 0.1 to 0.26 (Fig 3,2) and quantitatively higher (paired-t test, $p$= 0.04037) than to a T24 curve, which was 0.01 to 0.1 on average (Fig 3.2), with the exception of Per1, which had a better fit to the T24 curve and an $R^2$ value of 0.196. These data suggest that for 5 clock genes - Cry1, Cry2, Per2, Bmal1, and Clock - gene expression rhythmicity better fits an 18 hour curve than a 24 hour curve. Based on the aforementioned results and data from Chapter 2, it is likely that low goodness of fit to the sine curve may underlie the extraordinary flexibility of peripheral rhythms.

In order to examine the phase relationship between clock genes, we examined how the expression levels of each gene correlated with each other, and how the order of clock gene phases compared to the phase relationship of stably entrained controls. Correlations performed between gene expression levels of each clock gene revealed that Bmal1 expression is significantly correlated with Cry1 expression, Per2 expression is significantly correlated with Per1 and Cry2 expression, and Clock expression was significantly correlated with Bmal1 expression (Table 3.2). Interestingly, Per2 and Bmal1 were negatively correlated, but not in a statistically significant way. Strong correlations between Per2 and Cry2, Bmal1 and Clock, and Per1 and Per2 were all expected, but the strong positive correlation between Bmal1 and Cry1 was unexpected. These data indicate that the phase relationship between the core clock proteins is relatively preserved under entrainment to T18.

Peak phases of each clock gene expression were then compared to the phase of gene expression rhythms in the liver of mice stably entrained to T24, providing further insight into the preservation of the phase relationship. Under normal conditions, clock genes follow a specific temporal pattern that allows the transcription-translation feedback loop to function. Comparing the relative phase relationship to stably entrained controls allows for differentiation between which periodicity better reflects the rhythm we generate, 18 or 24 hours (Figure 3.3). When peak clock gene phases were normalized to the peak phases of T24 controls, the clustering of peak phases was stronger in T18 (Fig 3.3A) than T24 (Fig 3.3B), suggesting that the phase relationship plotted against an 18 hour sine curve is the better fit. Together, these data suggest that clock gene expression in the liver was cycling with rhythmicity closer to 18 hours than 24, as the phase relationship between clock genes is more preserved when analyzed as an 18 hour sine curve.

## DISCUSSION

With the implementation of T18 lighting and feeding cues, mice were capable of achieving entrainment to the shortened T cycle. Locomotor entrainment to T18 was fair, with about three quarters of the wheel running activity occurring during the dark phase, and a general decrease in the number of running wheel revolutions compared to stable entrainment in T24. With the implementation of an 18 hour TRF and an LD13:5 light cycle, we expected the two zeitgebers (light and food) to reinforce the strength of behavioral entrainment to T18, and were surprised to find out this was not the case. This may have been due to a change in cage geometry, as the cages used for food

restriction were narrower and were equipped with slower running wheels, and the feeding apparatus may have decreased the amount of light mice were exposed to. These results indicate that behaviorally, mice are capable of extraordinary entrainment to shortened T cycles of about 18 hours. While the mice were feeding ad libitum on LD13:5, we noted no observable 18 hour pattern in feeding, suggesting that feeding behavior may only entrained to T18 under a time restricted eating paradigm.

After two weeks under T18 and an 18 hour TRF, clock gene expression of the liver exhibits stronger signals of 18 hour rhythmicity than 24 hour rhythmicity, with the exception of one gene. While goodness of fit to a sine curve was relatively low across the board for both 18 and 24 hour sine curves, $R^2$ values tended to be stronger to an 18 hour curve. Correlations performed between clock gene expression levels provided supplementary information on whether an 18 or 24 hour period was more reasonable for the data we generated, and indicated a greater preservation of core clock gene phase when plotted against an 18 hour curve. When peak clock gene phases were normalized to the peak phases of T24 controls, the phase relationship on an 18 hour curve better reflects the phase relationship of clock genes that are stably entrained. Overall, these results indicate that rhythmicity of hepatic clock genes under 18 hour light and feeding cues more closely follow an 18 hour pattern, but we cannot say with certainty that a 24 hour rhythm is not present because there was still an amplitude and goodness of fit value when our data was compared to a 24 hour sine curve. Furthermore, gene expression levels do not necessarily reflect entrainment of clock genes, and may instead reflect induction or repression of clock genes by zeitgebers. As a result, some genes could potentially cycle on a 24 hour basis, while some cycle on an 18 hour basis.

In terms of hepatic clock gene expression, there were two possible outcomes: rhythms would be entrained to an 18 hour day, or they would free-run with a period of about 24 hours (Walkbeek, 2017). Thus, we were only able to determine whether clock gene expression rhythms under this alternative entrainment paradigm more closely matched an 18 or 24 hour rhythm. Hepatic gene expression rhythms could potentially exhibit competing rhythmicity at both periodicities if certain mice had peripheral rhythms that were well entrained and others that did not, as we noted in our locomotor assay. Our study examines hepatic clock gene expressions at a population level, so desynchrony between our samples may generate both 18 and 24 hour rhythmic signals (cite). Resolving whether or not there are multiple periodicities present would require examining an individual mouse over multiple time points. Additionally, T18 cycles in this study were given for 6 weeks, and in previous studies from our lab were only done for 11 days. The extended time frame in T18 may permit a free running rhythm to drift out of phase.

Given these data, the established lower range of entrainment for the hepatic clock likely spans to at least 18 hours. This flexibility may be enabled by the dampening of clock gene expression rhythms, as this was also observed in Chapter 2 (Watanbe, 2007). To expand knowledge on the limits of entrainment and circadian flexibility, future research could explore the molecular dynamics of induced circadian flexibility. Understanding the mechanism by which these circadian rhythms gain such extraordinary plasticity may provide insight as to how to reduce circadian disruption and increase circadian flexibility. Additionally, this study could be repeated using a T30 cycle to examine the upper limits of rhythm plasticity.

Chapter 3, in part is currently being prepared for submission for publication of the material. Koretoff, Alexandra. The thesis author was the primary researcher and author of this material.

## FIGURES

A

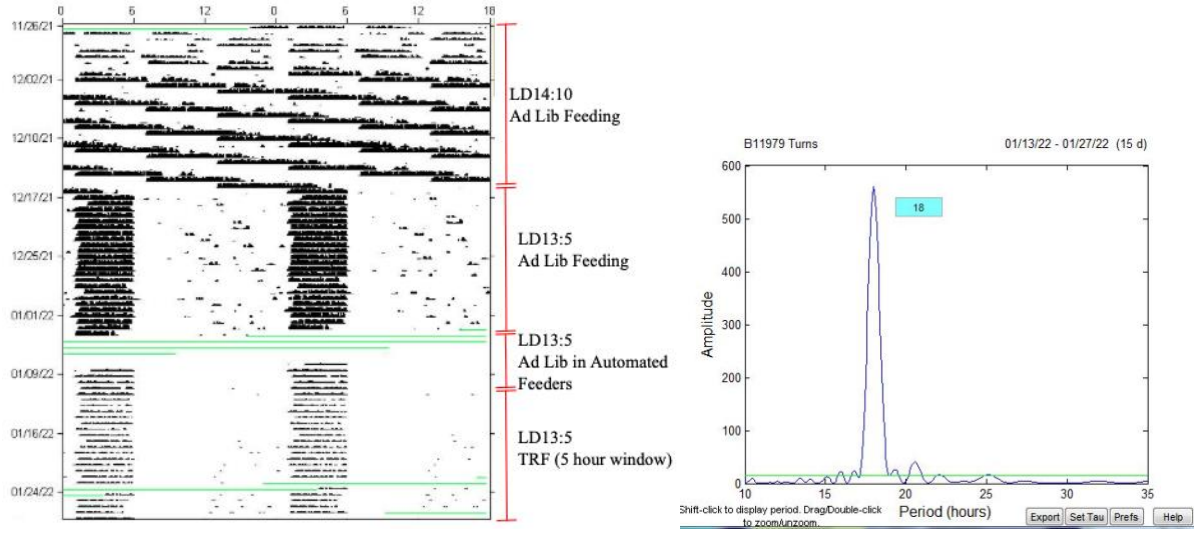


B

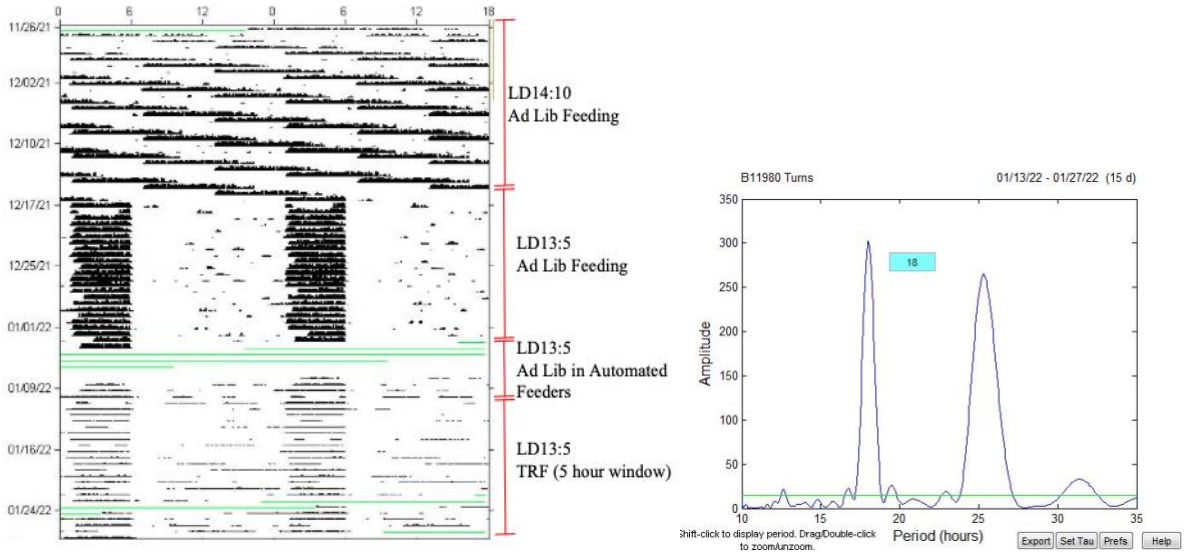


**Figure 3.1: Representative Actograms of T18 Behavioral Entrainment Status**
Representative double-plotted wheel running actograms (18 hr scale) and periodograms of (a) a mouse with locomotor activity well entrained to T18 (EQ= 0.98) and of (b) a mouse whose activity was not well entrained to T18 (EQ= .54). Wheel running activity is denoted by black tick marks and is plotted on an 18 hour basis. Red brackets indicate experimental conditions and duration of time mice were in those conditions. Green lines represent loss of wheel running data at those particular timepoints. Mice quickly entrained to T18 and ad libitum feeding from T24 with robust activity, which decreased when moved to the automated feeders. Mice entrained to T18 under a TRF to varying degrees.

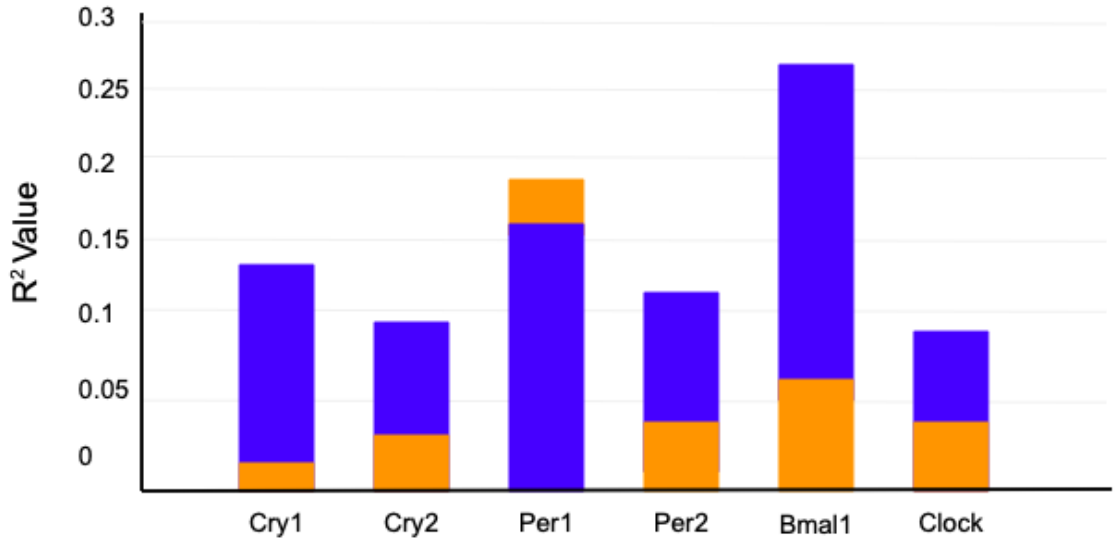


**Figure 3.2: Goodness of fit to T18 and T24 sine curves**
Column graphs depict the goodness of fit of clock gene expression to sine waves for each clock gene in the liver. Goodness of fit for each gene was generated from a least-squares regression in GraphPad Prism. Goodness of fit to an 18 hour sine wave is noted in blue while goodness of fit for a 24 hour sine curve is noted in orange. Goodness of fit was higher for an 18 hour curve, with the expectation of Per1.

| GENE | Cry1 | Cry2 | Per1 | Per2 | Bmal1 | Clock |
|---|---|---|---|---|---|---|
| Cry1 | 1 | 0.29397338 | 0.13547407 | 0.05080789 | 0.4736085 | -0.1901202 |
| Cry2 | | 1 | 0.21761805 | 0.39991624 | 0.17998138 | 0.32603798 |
| Per1 | | | 1 | 0.59394042 | 0.02100242 | -0.124157 |
| Per2 | | | | 1 | -0.2140315 | 0.07254813 |
| Bmal1 | | | | | 1 | 0.05427058 |
| Clock | | | | | | 1 |

**Table 3.2: Correlation coefficients between clock gene expression phases in T18**
Table listing the R-value generated by a Pearson correlation test between clock gene expression level between each gene, where a value of 1 or -1 is a perfect correlation and a value of 0 indicates no correlation. Statistically significant ($p<0.05$) relationships between phases of clock gene expression are highlighted in yellow. Statistically significant relationships between peak phases of gene expression between Per2 and Per1/Cry2, along with the weak negative correlation between Per2 and Bmal1, suggest partial preservation of stable phase relationships of clock genes.

A

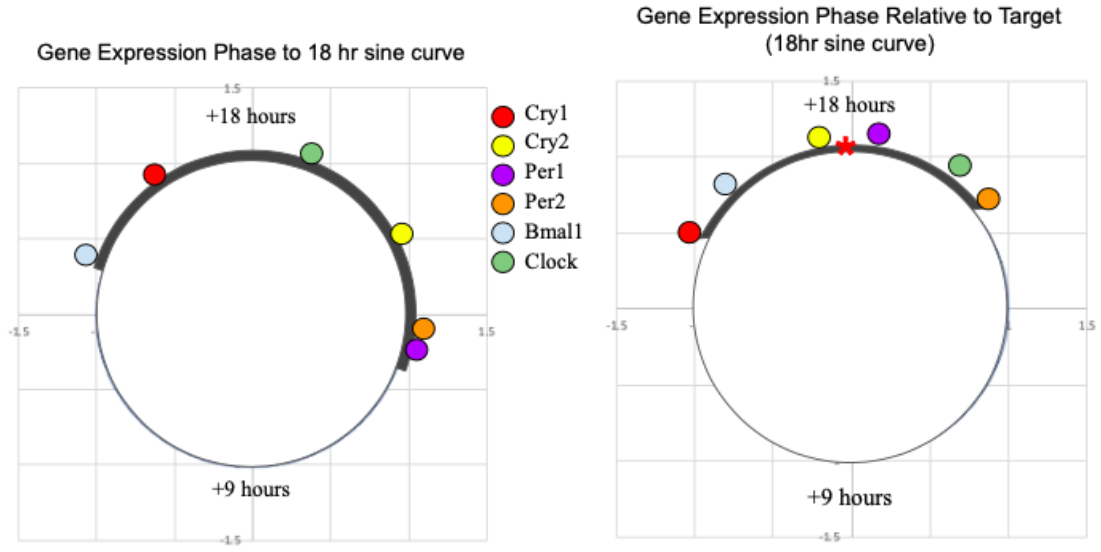


B

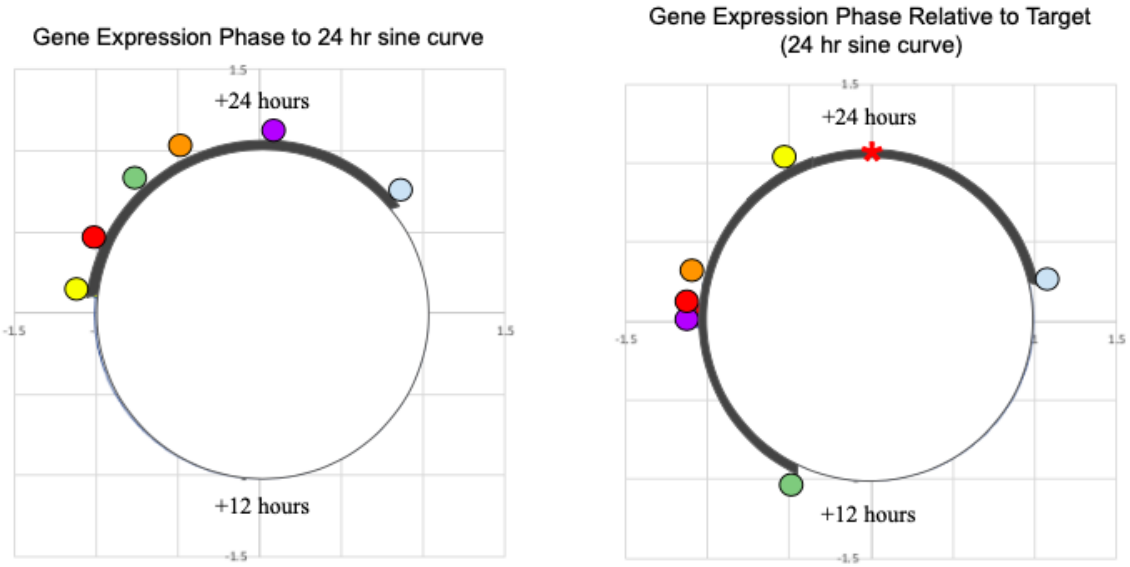


**Figure 3.3: Relative Phase to 18 and 24 hour sine curves**
Radial plots depicting the relative phase of clock gene transcripts in the liver for (a) a T18 sine curve and (b) a T24 sine curve. In (a) and (b), the radial plot on the left shows the order of peak phases compared to each other, and the radial plot on the right indicates the clock gene expression phase compared to the phase of a "stably entrained target" (asterisks). The white circle represents the amplitude at the value of "1". Black curves around the circle indicate the phase distribution of hepatic clock gene expression. A T18 curve better fits the data because the phase distribution is more similar to that of our controls.

## SI Figures

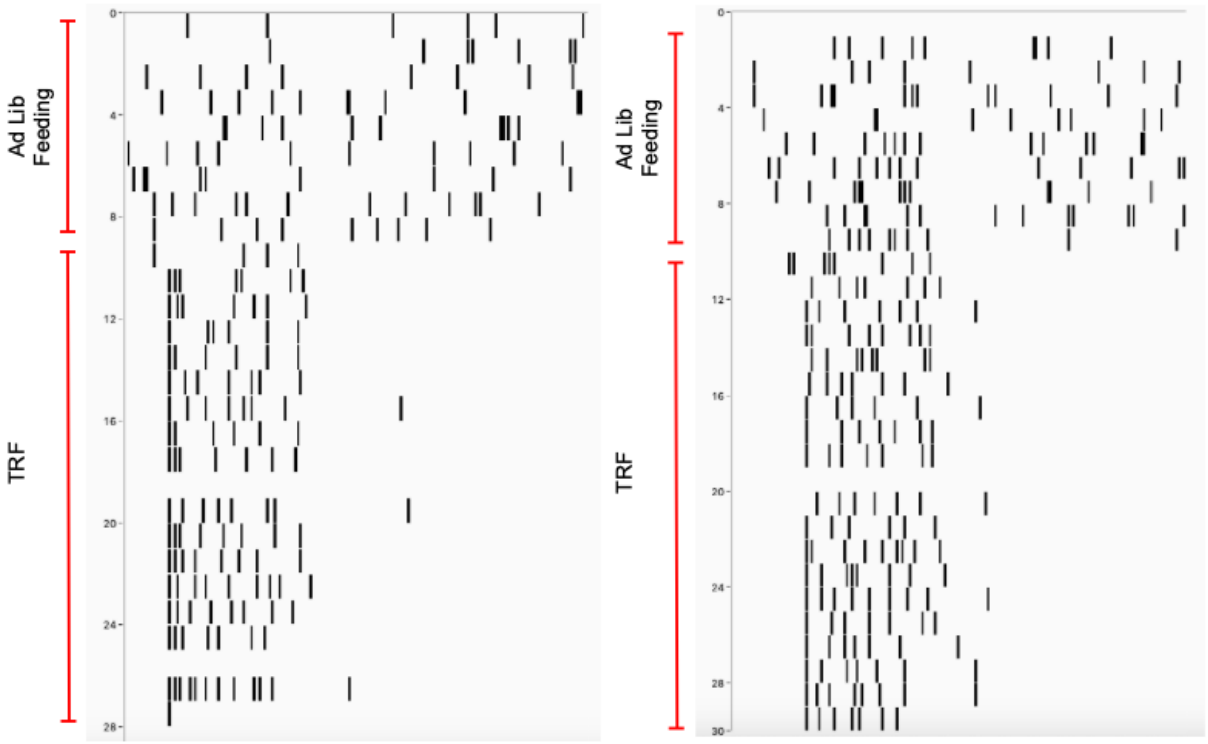


**Supplementary Figure 3.1: Actograms of Feeding Behavior**
Actograms showing feeding behavior were generated by ClockLab Analysis using feeder pellet collection data from our automated feeding system from Phenome Technologies. Black dashes indicate when a pellet was taken by the mouse. Red brackets indicate whether feeding was ad libitum or restricted to a certain window of time. During the ad libitum feeding phase, mice retrieved pellets around the clock with no discernable pattern until food restriction was initiated.

## References


Boulos Z, Rosenwasser AM, Terman M. Feeding schedules and the circadian organization of behavior in the rat. Behav Brain Res. 1980 Feb;1(1):39-65. doi: 10.1016/0166-4328(80)90045-5. PMID: 7284080.

Carneiro, Breno T S, and John F Araujo. “Food entrainment: major and recent findings.” *Frontiers in behavioral neuroscience* vol. 6 83. 27 Nov. 2012, doi:10.3389/fnbeh.2012.00083

Chaix, Amandine & Zarrinpar, Amir & Satchidananda, Panda. “The circadian coordination of cell biology.” *The Journal of cell biology* vol. 215,1 (2016): 15-25. doi:10.1083/jcb.201603076

Duffy JF, Czeisler CA. Effect of Light on Human Circadian Physiology. Sleep Med Clin. 2009 Jun;4(2):165-177. doi: 10.1016/j.jsmc.2009.01.004. PMID: 20161220; PMCID: PMC2717723.

Dunlap JC. 1999. Molecular bases for circadian clocks. *Cell* 96:271–90, ISSN 0092-8674, https://doi.org/10.1016/S0092-8674(00)80566-8.

Evans, Jennifer & Elliott, Jeffrey & Gorman, MR. (2011). Dim Nighttime Illumination Interacts With Parametric Effects of Bright Light to Increase the Stability of Circadian Rhythm Bifurcation in Hamsters. Chronobiology international. 28. 488-96. 10.3109/07420528.2011.591952.

Gorman MR, Elliott JA. Entrainment of 2 subjective nights by daily light:dark:light:dark cycles in 3 rodent species. J Biol Rhythms. 2003 Dec;18(6):502-12. doi: 10.1177/0748730403260219. PMID: 14667151.

Hamaguchi, Yutaro & Tahara, Yu & Hiro, Kuroda & Atsushi, Haragushi & Shibata, Shigenobu. “Entrainment of mouse peripheral circadian clocks to <24 h feeding/fasting cycles under 24 h light/dark conditions.” *Scientific reports* vol. 5 14207. 23 Sep. 2015, doi:10.1038/srep14207

Harrison, EM, Walbeek T, & Sun J, Johnson, J, Poonawala Q, Gorman, MR. “Extraordinary behavioral entrainment following circadian rhythm bifurcation in mice.” *Scientific reports* vol. 6 38479. 8 Dec. 2016, doi:10.1038/srep38479

Harrison EM, Gorman MR. Rapid Adjustment of Circadian Clocks to Simulated Travel to Time Zones across the Globe. J Biol Rhythms. 2015 Dec;30(6):557-62. doi: 10.1177/0748730415598875. Epub 2015 Aug 14. PMID: 26275871.

Husse J, Leliavski A, Tsang AH, Oster H, Eichele G. The light-dark cycle controls peripheral rhythmicity in mice with a genetically ablated suprachiasmatic nucleus clock. FASEB J. 2014 Nov;28(11):4950-60. doi: 10.1096/fj.14-256594. Epub 2014 Jul 25. PMID: 25063847.

Johnson C, Elliott J, Foster R. (2003). Entrainment of Circadian Programs. Chronobiology International, 20(5), 741–774. doi:10.1081/CBI- 120024211

Kori H, Yamaguchi Y, Okamura H. Accelerating recovery from jet lag: prediction from a multi-oscillator model and its experimental confirmation in model animals. *Sci Rep* 7, 46702 (2017). https://doi.org/10.1038/srep46702

Livak KJ, Schmittgen TD. Analysis of relative gene expression data using real-time quantitative PCR and the 2(-Delta C(T)) Method. Methods. 2001 Dec;25(4):402-8. doi: 10.1006/meth.2001.1262. PMID: 11846609.

Mistlberger, R. (1990). Circadian pitfalls in experimental designs employing food restriction. *Psychobiology, 18*(1), 23–29.

Nicholls SK, Casiraghi LP, Wang W, Weber ET, & Harrington ME. “Evidence for Internal Desynchrony Caused by Circadian Clock Resetting.” *The Yale journal of biology and medicine* vol. 92,2 259-270. 27 Jun. 2019

Noguchi T, Harrison EM, Sun J, May D, Ng A, Welsh DK, Gorman MR. Circadian rhythm bifurcation induces flexible phase resetting by reducing circadian amplitude. Eur J Neurosci. 2020 Jun;51(12):2329-2342. doi: 10.1111/ejn.14086. Epub 2018 Aug 16. PMID: 30044021.

Pfaffl, M W. “A new mathematical model for relative quantification in real-time RT-PCR.” *Nucleic acids research* vol. 29,9 (2001): e45. doi:10.1093/nar/29.9.e45

Potter GD, Skene DJ, Arendt J, Cade JE, Grant PJ, Hardie LJ. Circadian Rhythm and Sleep Disruption: Causes, Metabolic Consequences, and Countermeasures. Endocr Rev. 2016 Dec;37(6):584-608. doi: 10.1210/er.2016-1083. Epub 2016 Oct 20. PMID: 27763782; PMCID: PMC5142605.

Ralph, Martin R., Michael Menaker. “A Mutation of the Circadian System in Golden Hamsters.” *Science*, vol. 241, no. 4870, 1988, pp. 1225–1227., https://doi.org/10.1126/science.3413487.

Reppert, Steven M, David R Weaver. “Molecular Analysis of Mammalian Circadian Rhythms.” *Annual Review of Physiology*, vol. 63, no. 1, Mar. 2001, pp. 647–676., https://doi.org/10.1146/annurev.physiol.63.1.647.

Rosenwasser AM, Pelchat RJ, Adler NT. (1984). Memory for feeding time: Possible dependence on coupled circadian oscillators. *Physiology & Behavior, 32*(1), 25–30. https://doi.org/10.1016/0031-9384(84)90064-7

Rosenwasser AM, Turek FW. Neurobiology of Circadian Rhythm Regulation. Sleep Med Clin. 2015 Dec;10(4):403-12. doi: 10.1016/j.jsmc.2015.08.003. Epub 2015 Sep 11. PMID: 26568118

Snyder, Cynthia K., Anne-Marie Chang. “Mobile Technology, Sleep, and Circadian Disruption.” *Sleep and Health*, 19 Apr. 2019, pp. 159–170., https://doi.org/10.1016/b978-0-12-815373-4.00013-7.

Stubblefield J.J., Green C.B. (2016). Mammalian Circadian Clocks and Metabolism: Navigating Nutritional Challenges in a Rhythmic World. In: Gumz, M. (eds) Circadian Clocks: Role in Health and Disease. Physiology in Health and Disease. Springer, New York, NY. https://doi.org/10.1007/978-1-4939-3450-8_5

Tahara, Yu, Shigenobu Shibata. “Circadian rhythms of liver physiology and disease: experimental and clinical evidence.” *Nature reviews. Gastroenterology & hepatology* vol. 13,4 (2016): 217-26. doi:10.1038/nrgastro.2016.8

Tao W, Wu J, Zhang Q, Lai S, Jiang S, Jiang C, Xu Y, Xue B, Du J, Li CJ. “EGR1 regulates hepatic clock gene amplitude by activating Per1 transcription.” *Scientific reports* vol. 5 15212. 16 Oct. 2015, doi:10.1038/srep15212

Trott, Alexandra J, Jerome S Menet. “Regulation of circadian clock transcriptional output by CLOCK:BMAL1.” *PLoS genetics* vol. 14,1 e1007156. 4 Jan. 2018, doi:10.1371/journal.pgen.1007156

Vollmers C, Gill S, DiTacchio L. “Time of feeding and the intrinsic circadian clock drive rhythms in hepatic gene expression.” *Proceedings of the National Academy of Sciences of the United States of America* vol. 106,50 (2009): 21453-8. doi:10.1073/pnas.0909591106

Walbeek T, Harrison EM, Soler R, Gorman MR. “Enhanced Circadian Entrainment in Mice and Its Utility under Human Shiftwork Schedules.” *Clocks & sleep* vol. 1,3 394-413. 26 Aug. 2019, doi:10.3390/clockssleep1030032

Walbeek TJ, Gorman MR. Simple Lighting Manipulations Facilitate Behavioral Entrainment of Mice to 18-h Days. *Journal of Biological Rhythms*. 2017;32(4):309-322. doi:10.1177/0748730417718347

Watanabe T, Naito E, Nakao N, Tei H, Yoshimura T, Ebihara S. Bimodal Clock Gene Expression in Mouse Suprachiasmatic Nucleus and Peripheral Tissues Under a 7-Hour Light and 5-Hour Dark Schedule. *Journal of Biological Rhythms*. 2007;22(1):58-68. doi:10.1177/0748730406295435

Welsh D, Takahashi JS, Kay SA. “Suprachiasmatic nucleus: cell autonomy and network properties.” *Annual review of physiology* vol. 72 (2010): 551-77. doi:10.1146/annurev-physiol-021909-135919

West, Alexander C., Bechtold David A. "The cost of circadian desynchrony: Evidence, insights and open questions." *Bioessays* 37.7 (2015): 777-788.

Yamajuku D, Inagaki T, Haruma T. Real-time monitoring in three-dimensional hepatocytes reveals that insulin acts as a synchronizer for liver clock. *Sci Rep* 2, 439 (2012). https://doi.org/10.1038/srep00439

Yan L, Silver R, Gorman M. Reorganization of Suprachiasmatic Nucleus Networks under 24-h LDLD Conditions. *Journal of Biological Rhythms*. 2010;25(1):19-27. doi:10.1177/0748730409352054